

ON MOVES BETWEEN BRANCHED COVERINGS OF S^3 THE CASE OF FOUR SHEETS

NIKOS APOSTOLAKIS

ABSTRACT. A combinatorial presentation of closed orientable 3-manifolds as bi-tricolored links is given together with two versions of a calculus via moves to manipulate bi-tricolored links without changing the represented manifold. That is, we provide a finite set of moves sufficient to relate any two manifestations of the same 3-manifold as a simple 4-sheeted branched covering of S^3 .

CONTENTS

0. Introduction	2
1. Preliminaries	3
1.1. Generalities	3
1.2. Branched coverings over D^2	4
1.3. Coverings over S^3	10
1.4. Dimming the lights	12
1.5. Adding a trivial sheet	13
2. The 3-sheeted case	13
2.1. 3-sheeted Coverings of S^2	13
2.2. 3-sheeted Coverings of S^3	16
3. Four sheets I: Coverings over S^2	20
3.1. The Complex	21
3.2. Generators	27
3.3. The Kernel	38
4. Four sheets II: Coverings over S^3	41
4.1. Bi-tricolored links	41
4.2. Moves	41
5. Some Open Questions	57
Appendix A. Wajnryb's presentation of \mathfrak{M}_g	58
Appendix B. Braids	59
Appendix C. Link diagrams	60
Appendix D. Heegaard splittings	60
References	63

1991 *Mathematics Subject Classification*. Primary 57M12; Secondary 57M25.

Key words and phrases. branched covering, covering move, colored braid, colored link, 3-manifold.

A major part of this work was completed at the Graduate Center of CUNY as part of the authors doctoral dissertation.

0. INTRODUCTION

It is known that every oriented 3-dimensional manifold manifests itself as (the total space of) a branched covering over the 3-dimensional sphere S^3 , with simple branching behaviour ([1]). Furthermore it is known that the degree of the covering can be chosen to be any natural number greater or equal to three ([8], [9]). This fact leads to a combinatorial presentation of 3-manifolds via colored link diagrams, that is diagrams of (planar projections of) links whose arcs are labeled by transpositions of some symmetric group. The following question then arises:

Find a finite set of (preferably local) moves, such that any two presentations of the same 3-manifold as a colored link can be related by a finite sequence of moves from this set.

By a local move we vaguely mean a move that applies to a relatively small part of the diagram independently of the structure of the link outside that part. We don't attempt to give a more precise meaning to the term local move.

In this study we concentrate on coverings of degree 4 and give two answers:

Theorem 4.2.1 gives a set of five moves (two local and three non local) sufficient to relate any two presentations of the same manifold as a 4-sheeted simple branched covering of the 3-sphere.

Theorem 4.2.2 proves that after adding a fifth sheet in a standard way the two local moves of Theorem 4.2.1 suffice.

These results and their proofs are modeled on similar results of Piergallini for coverings of degree 3 ([11], [12]). It is unknown at this time if similar results are true for coverings of degree greater or equal to 5.

The rest of this work is organized as follows:

Section 1 sets the stage: Basic definitions are given and basic results are stated (and sometimes proved) to be used in the later sections.

Section 2 reviews, for the sake of completeness, what is known for simple branched coverings of degree 3. We emphasize that all results in this section have been discovered by other people. In particular subsection 2.1 summarizes the relevant results of [4] and subsection 2.2 the results of [11] and [12].

In Section 3 the main technical results of this work are proved. We study simple 4-sheeted coverings of the 2-sphere and the braid group action on them. This section culminates with Theorem 3.3.2 in which normal generators for the kernel of the quotiented lifting homomorphism are given.

In Section 4 the above mentioned results about moves are proved.

Section 5 concludes this work by asking some questions that arise in the course of our study.

Finally, to fix conventions etc., we sketch in four Appendices background material that is used throughout this work.

1. PRELIMINARIES

In what follows we always work in the PL category. Thus manifold means PL manifold, submanifold means locally flat submanifold, homeomorphism means PL homeomorphism, etc.

1.1. **Generalities.** Lets begin with the basic definitions:

Definition 1.1.1. A *branched covering* $p : E(p) \rightarrow B(p)$ is a surjective map between manifolds such that there is a codimension-2 submanifold L of $B(p)$ with the property that p restricted to the preimage of $B(p) \setminus L$ is a finite covering. p is called the (covering) projection, $E(p)$ the total space, $B(p)$ the base space and L the (downstairs) branching locus.

If the base space B has a basepoint $* \notin L$ then an m -sheeted *pointed* branched covering of B is an m -sheeted branched covering together with an identification of $p^{-1}(*)$ with $\{1, \dots, m\}$.

An *equivalence* between branched coverings is a commutative diagram

$$\begin{array}{ccc} E(p_1) & \xrightarrow{f} & E(p_2) \\ p_1 \downarrow & & \downarrow p_2 \\ B(p_1) & \xrightarrow{\bar{f}} & B(p_2) \end{array}$$

where f, \bar{f} are homeomorphisms. \bar{f} is said to *cover*, or to be *over*, or to *lift* f .

An equivalence between pointed branched coverings is a commutative diagram as above with \bar{f} basepoint preserving and f commuting with the identifications of the fibers with $\{1, \dots, m\}$. Such an f is called *pointed*.

An *isomorphism* of (pointed) branched coverings is an equivalence over the identity.

Remark 1.1.2. A much more general definition of branched coverings can be found in [7].

Proposition 1.1.3. *Let M be a manifold and L a codimension-2 submanifold of M . Then:*

*Equivalence classes of pointed m -sheeted coverings of M branched over L are in bijection with $\text{Hom}(\pi_1(M \setminus L, *), \mathcal{S}_m)$, where \mathcal{S}_m denotes the symmetric group on m symbols.*

*Equivalence classes of (unpointed) m -sheeted coverings of M branched over L are in bijection with $\text{Hom}(\pi_1(M \setminus L, *), \mathcal{S}_m)/\mathcal{S}_m$, where \mathcal{S}_m acts by conjugation in the range.*

The pullback of a (pointed) branched covering by a homeomorphism is again a (pointed) branched covering branched over the preimage of the branching locus. The above bijections are equivariant with respect to pullbacks.

Proof. Fox proved in [7] that a branched covering is determined, up to equivalence, by its restriction outside the branching locus and that any finite covering of $B \setminus L$ can be extended to a branched covering of B . Applying the standard theory of covering spaces one gets the result. \square

The homomorphism $\rho : \pi_1(M \setminus L, *) \rightarrow \mathcal{S}_m$ corresponding to p is called the *monodromy* of p . From now on a branched covering will systematically be confused with its monodromy in the sense that the same symbol will be used for both.

The following holds:

Lemma 1.1.4. *Let $p : \widetilde{M} \rightarrow M$ be a pointed branched covering and $h : M \rightarrow M$ a based homeomorphism that fixes the branching locus as a set. Then h lifts to a pointed equivalence of $\tilde{h} : \widetilde{M} \rightarrow \widetilde{M}$ iff the pullback $h^*(p)$ is isomorphic to p .*

Proof. Consider the following commutative diagram:

$$\begin{array}{ccccc}
 & & \phi & & \\
 & & \curvearrowright & & \\
 h^*(\widetilde{M}) & \xrightarrow{h^*} & \widetilde{M} & \xrightarrow{\tilde{h}^{-1}} & \widetilde{M} \\
 h^*p \downarrow & & p \downarrow & & p \downarrow \\
 M & \xrightarrow{h} & M & \xrightarrow{h^{-1}} & M \\
 & & \text{id} & &
 \end{array}$$

Obviously one of the dotted arrows exists iff the other does. \square

Notice that \tilde{h} is unique (when it exists).

Definition 1.1.5. An m -sheeted branched covering is called simple if the preimage of any point has cardinality at least $m - 1$.

1.2. Branched coverings over D^2 . From now on, unless explicitly mentioned otherwise, covering will mean a *branched* covering. Although we are mainly interested in coverings over the sphere S^2 it is convenient to consider coverings over the disc D^2 .

To set the stage consider D^2 as the unit disk in \mathbb{C} with basepoint $* = -1$. The branching locus L of a covering will be a finite set of points, $L = \{A_0, A_1, \dots, A_{n-1}\}$, which are assumed to lie in the real axis in that order. $\pi_1(D^2 \setminus L, *)$ is a free group on the generators $\alpha_0, \alpha_1, \dots, \alpha_{n-1}$, where α_i is represented by a *lasso* based at $*$ and going around A_i in the counterclockwise direction as shown in Figure 1.

Then using Proposition 1.1.3 one can represent an m -sheeted pointed covering branched over L as a sequence of permutations $\sigma_0, \sigma_1, \dots, \sigma_{n-1}$ of \mathcal{S}_m , where such a sequence represents the covering

$$\begin{aligned}
 \rho : \pi_1(D^2 \setminus L, *) &\longrightarrow \mathcal{S}_m \\
 \rho(\alpha_i) &= \sigma_i \quad \text{for } i = 0, \dots, n-1
 \end{aligned}$$

Such a sequence represents a simple covering iff all σ_i 's are transpositions. Unless explicitly mentioned otherwise *all coverings are assumed simple and pointed* from now on.

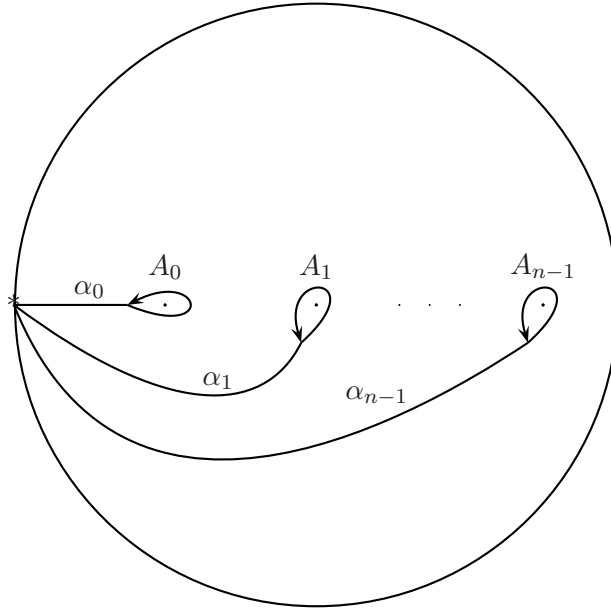
Coverings of S^2 The number of boundary components of the total space of ρ equals the number of cycles (including cycles of length 1) in a decomposition of

$$\sigma = \prod_{i=0}^{n-1} \sigma_i$$

into disjoint cycles. Indeed σ is the monodromy around the (positively oriented) boundary.

In particular if $\sigma = \text{id}$, $E(\rho)$ has m boundary components, each mapping homeomorphically onto ∂D^2 . Thus one can “fill them in” with m discs to get a covering of

$$S^2 = D^2 \bigcup_{\partial D^2} D^2$$

FIGURE 1. The free generators of $\pi_1(D^2 \setminus L, *)$

with each filled in disk mapping homeomorphically onto the second D^2 . Conversely given a covering of S^2 one can cut off a disk not containing any branch values to get a covering of a disk with boundary monodromy equal to id. Thus coverings of D^2 with identity boundary monodromy can (and will) be identified with coverings of S^2 .

If ρ is a covering of S^2 the Euler characteristic of $E(\rho)$ can be calculated by choosing compatible triangulations upstairs and downstairs. One gets the following version of the Riemann-Hurwitz formula:

$$(1.2.1) \quad \chi(E(\rho)) = 2m - n$$

where m is the degree and n the number of branch values. As a corollary the number of branch values is even. In terms of genus (assuming that $E(\rho)$ is connected):

$$(1.2.2) \quad g(E(\rho)) = \frac{n}{2} - m + 1 \quad .$$

Constructing branched coverings by cutting and pasting. There is a well known method (going back to Riemann) for getting models for coverings over D^2 by “cutting and pasting”. Let $\rho = \sigma_0, \sigma_1, \dots, \sigma_{n-1}$ be a, not necessarily simple, m -sheeted covering of D^2 branched over L . For $i = 0, 1, \dots, n - 1$ take an arc γ_i connecting the branching value A_i to a boundary point (other than the basepoint $*$), in such a way that two different γ_i 's are disjoint. Cut the disc along these arcs to get a new disk with $2n$ distinguished arcs on its boundary: each γ_i gives two arcs joined at A_i , call these two arcs γ_i^0 and γ_i^1 . Now take m copies of the cut disc (the sheets of the covering) numbered 1 through m and glue them along their distinguished arcs according to the σ_i 's, that is for $i = 0, 1, \dots, n - 1$ and $j = 1, \dots, m$ glue the j -th copy of γ_i^0 to the $\sigma_i(j)$ -th copy of γ_i^1 . The result of these

gluings is the total space of the covering. The projection is the obvious one. See Figure 4 for an example of this construction.

Notice that since the cuts described above make $D^2 \setminus L$ simply connected (in fact contractible) this method can be used to construct a model for *any* covering of D^2 branched over L . However in order to construct a given covering one can cut along any 1-dimensional subcomplex of $D^2 \setminus L$ as long as the fundamental group of the cut disk is sent to identity by the monodromy of the covering. This observation will be used later when we will construct specific coverings of the 2-dimensional sphere.

The Braid group action. See Appendix B for the definition of the braid group B_n . It is known that the group $\mathfrak{M}_{0,1,n}$ of isotopy classes of homeomorphisms of $(D^2, L, \text{rel } \partial D^2)$, is isomorphic with B_n the braid group on n strands (see for example [3]). The isomorphism is given by sending the generator β_i of B_n to (the isotopy class of) the rotation around the interval x_i for $i = 0, \dots, n-1$, where x_i is the interval between A_i and A_{i+1} on the real axis. In general

Definition 1.2.1. An interval is a path x in the interior of D^2 with endpoints in L but otherwise missing L .

A rotation around x is a homeomorphism that fixes pointwise the complement of a disc neighborhood U of x in $D^2 \setminus L$ while rotating the interior of U by 180° counterclockwise, mapping x to itself with its endpoints reversed (see Figure 2). The class in $\mathfrak{M}_{0,1,n}$ of a rotation around an interval x depends only on the isotopy class rel endpoints of x and is denoted by β_x .

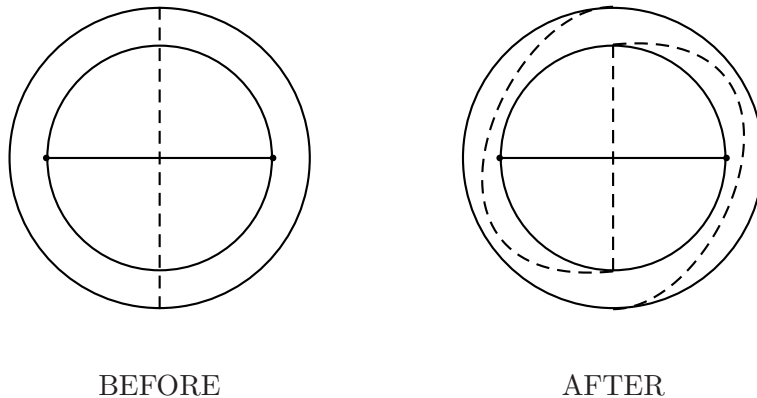


FIGURE 2. Rotation around an interval.

A braid will be confused with its image on $\mathfrak{M}_{0,1,n}$ but all the induced actions of B_n are considered *right* actions. In particular B_n acts on the right on

- $\pi_1(D^2 \setminus L, *)$.

This action is given by

$$(\alpha_j)\beta_i = \begin{cases} \alpha_j & \text{if } j \neq i, i+1, \\ \alpha_{i+1} & \text{if } j = i, \\ \alpha_{i+1}\alpha_i\alpha_{i+1}^{-1} & \text{if } j = i+1. \end{cases} \quad \text{for } i, j = 0, \dots, n-1.$$

- Isotopy classes of intervals.

This action has the property

$$\beta_{(x)\beta} = \beta^{-1}\beta_x\beta \quad \forall \text{ intervals } x, \forall \beta \in B_n \quad .$$

Notation: For two braids β, β' denote $\beta^{-1}\beta'\beta$ by $[\beta']\beta$, so that the rotation around the interval $(x)\beta$ is denoted by $[\beta_x]\beta$.

- $\text{Hom}(\pi_1(D^2 \setminus L, *), \mathcal{S}_m)$.

This action is defined by:

$$((\rho)\beta)(\alpha) = \rho(\alpha\beta^{-1})$$

and corresponds to pullback of coverings by homeomorphisms (which act on the left).

This last action of B_n can be expressed combinatorially via “colored braids”. Represent a covering ρ as a “coloring” of the branching locus L , i.e. as a labelling of A_i ’s by transpositions of the symmetric group \mathcal{S}_m (referred to as colors). To see how a braid β acts on ρ draw a diagram of β with its top endpoints coinciding with L , and let the colors of ρ “flow down” through the diagram according to the rule that when a strand passes under another strand its color gets conjugated by the color of the over strand. That way we get a new coloring of L at the bottom of the diagram. This bottom coloring represents $(\rho)\beta$. Figure 3 shows the action of a generator in the cases that the top colors coincide, “intersect”, or are disjoint, respectively.

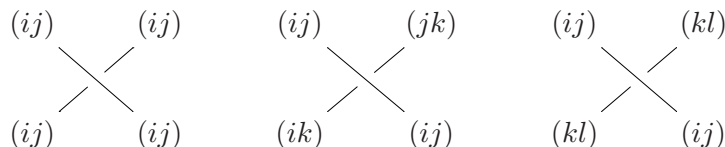


FIGURE 3. How a generator of B_n acts.

The Category of Colored Braids. The above can be said in a categorical language, with colorings of L being objects and colored braids being morphisms. Then we have a “lifting functor” from the category of colored braids to the category with objects coverings of D^2 branched over L and morphisms equivalences between them. Indeed it follows from Lemma 1.1.4 that (the isotopy class of) the homeomorphism corresponding to a colored braid lifts to an equivalence between the coverings corresponding to its ends. In particular there is a lifting homomorphism

$$\lambda(\rho) : \text{Aut}(\rho) \longrightarrow \mathfrak{M}(E(\rho))$$

where \mathfrak{M} denotes the mapping class group and $\text{Aut}(\rho)$ denotes the group of automorphisms of ρ as an object in this category. By Lemma 1.1.4 $\text{Aut}(\rho)$ consists of those braids that lift to isomorphisms of ρ .

The following lemma describes the “lifting status” of rotations around intervals.

Lemma 1.2.2. *Let x be an interval and α an element of $\pi_1(D^2 \setminus L, *)$ represented by a path that goes around one of the endpoints of x and meets x only once. Then:*

- (a) *If $\rho(\alpha\beta_x) = \rho(\alpha)$ then $p^{-1}(x)$ consists of a loop and $m - 2$ arcs mapping homeomorphically onto x . A rotation around x will then lift to the composition of a Dehn twist around the loop and rotations around the arcs, so that β_x lifts to a Dhen twist around the loop.*
- (b) *If $\rho(\alpha\beta_x)$ and $\rho(\alpha)$ are intersecting transpositions then $p^{-1}(x)$ consists of a “length 3” arc and $m - 3$ arcs mapping homeomorphically onto x . Then β_x doesn’t lift but β_x^3 lifts to id.*
- (c) *If $\rho(\alpha\beta_x)$ and $\rho(\alpha)$ are disjoint transpositions then $p^{-1}(x)$ consists of two “length 2” arcs and $m - 4$ arcs mapping homeomorphically onto x . Then β_x doesn’t lift but β_x^2 lifts to id.*

Proof. Assume without loss of generality, that the subgroup of \mathbb{S}_n generated by the monodromies of α , $\alpha\beta_x$ fixes the complement of $\{1, 2, 3, 4\}$. Take a disk neighborhood U of $x \cup \alpha$ that contains $\alpha\beta_x$ and misses all branch values except the endpoints of x (clearly such a neighborhood exists). The restriction of p in U is obviously equivalent to one of the following three coverings

- (a) (12), (12)
- (b) (12), (23)
- (c) (12), (24)

via an equivalence that sends x to x_0 and α , $\alpha\beta_x$ to α_0 , α_1 . The proof then reduces to verifying the statements for those three coverings. For this see Figure 4, which gives explicit models of these coverings constructed by cutting and pasting. The intervals and their lifts are shown in yellow while the cuts are shown in grey. It is to be understood that the “free” grey arcs are “folded in half”. Using this picture one can easily check by projecting that the maps lift as claimed. \square

Consider the moves between colored braids shown in Figures 5 and 6. It should be emphasized that in this section they are considered as moves between braid diagrams, that is the strands are always *vertical*.

Let $N(\rho)$ be the set of colored braids that can be related to the identity automorphism of ρ , that is the identity braid colored by the colors of ρ , via a finite sequence of these two moves. Since both moves are local it is clear that $N(\rho)$ is a normal subgroup of $\text{Aut}(\rho)$ and furthermore it is natural, that is if $\rho\beta = \rho'$ then $N(\rho') = \beta^{-1}N(\rho)\beta$.

Definition 1.2.3.

$$\overline{\text{Aut}}(\rho) = \frac{\text{Aut}(\rho)}{N(\rho)}$$

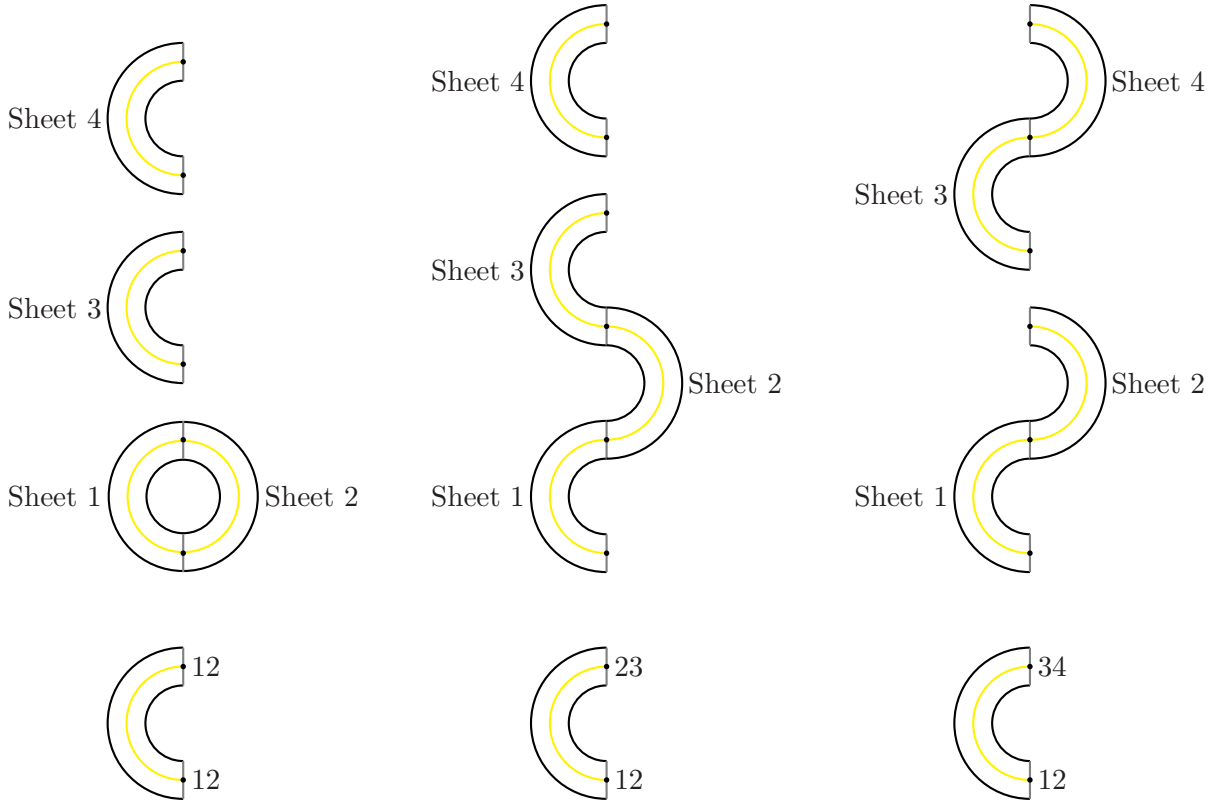


FIGURE 4. How various intervals lift

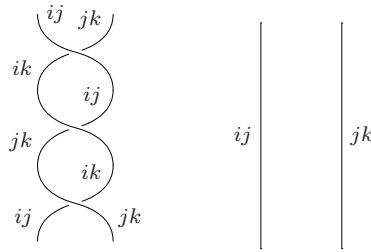
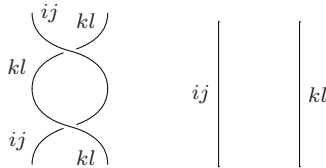


FIGURE 5. Move \mathcal{M}

By Lemma 1.2.2, $N \triangleleft \text{Ker}(\lambda(\rho))$ and therefore the lifting homomorphism $\lambda(\rho)$ descends to a homomorphism $\bar{\lambda}(\rho) : \overline{\text{Aut}}(\rho) \rightarrow \mathfrak{M}(E(\rho))$, that is, there is a commutative diagram:

$$(1.2.3) \quad \begin{array}{ccc} \text{Aut}(\rho) & \xrightarrow{\lambda(\rho)} & \mathfrak{M}(E(\rho)) \\ \downarrow & \nearrow \bar{\lambda}(\rho) & \\ \overline{\text{Aut}}(\rho) & & \end{array}$$

FIGURE 6. Move \mathcal{P}

1.3. Coverings over S^3 . Consider an m -sheeted covering of S^3 . The branching locus will be a codimension-2 submanifold of S^3 that is a link L . According to Proposition 1.1.3 the covering is determined by its monodromy. The total space of the covering is connected iff the image of the monodromy homomorphism is a transitive subgroup of \mathcal{S}_m . From now on unless explicitly mentioned otherwise *the total space of a covering will always be assumed connected*. Recall that coverings are assumed to be simple which in this context means that the monodromy associated to each Wirtinger generator is a transposition.

Definition 1.3.1. An m -colored link is a link L together with a simple, transitive representation of its group $\pi_1(S^3 \setminus L)$ into the symmetric group \mathcal{S}_m . A 3-colored link will be called tricolored and a 4-colored link will be called bi-tricolored.

Given an isotopy between two links there is an induced isomorphism between their groups (see Appendix C). Therefore an isotopy between two links induces a bijection between their colorings.

Definition 1.3.2. Two colored links are called *color-isotopic* (or when there is no danger of confusion just isotopic) if there exists an isotopy between them that transforms the coloring of one link to the coloring of the other link.

Recall (see Appendix C) that given a diagram of a link there is an associated Wirtinger presentation of the link group with a generator for each arc of the diagram and a relation for each crossing. Therefore an m -colored link can be represented combinatorially by an m -colored diagram that is a link diagram with its arcs labelled with transpositions of \mathcal{S}_m in a manner compatible with the Wirtinger presentation. Specifically:

Definition 1.3.3. An m -colored link diagram is a link diagram with its arcs labelled by transpositions of \mathcal{S}_m in such a way that the subgroup of \mathcal{S}_m generated by all the labels is transitive, and furthermore at each crossing the transposition labelling one of the under arcs equals the transposition of the other under arc conjugated by the transposition of the over arc.

A colored link diagram obviously represents a colored link. Call two colored link diagrams equivalent if they represent isotopic colored links.

Remark 1.3.4. By looking at how Reidemeister moves transform the presentations of the link group (see Remark C.0.12) one can define colored Reidemeister moves and prove that two colored link diagrams are equivalent iff they can be related by a finite sequence of colored Reidemeister moves.

Definition 1.3.5. An m -colored link presentation of a 3-manifold M is an m -colored link diagram L , such that M is homeomorphic to $E(\rho)$. In this case one writes $M = M(L)$ and says that M is represented by L .

Plat diagrams and Heegaard splittings. One way to understand the manifold represented by a colored link diagram is the following: Start with a plat diagram of the colored link (see for example [3] for a proof of the fact that each link has a plat diagram), that is a braid diagram closed on its top and bottom by caps and cups and split the three-sphere S^3 as

$$S^3 = D_1 \cup S^2 \times I \cup D_2$$

where D_1 is a 3-dimensional disc containing all the caps, D_2 is a 3-dimensional disc containing all the cups, and the braid is contained in $S^2 \times I$ as shown in Figure 7.

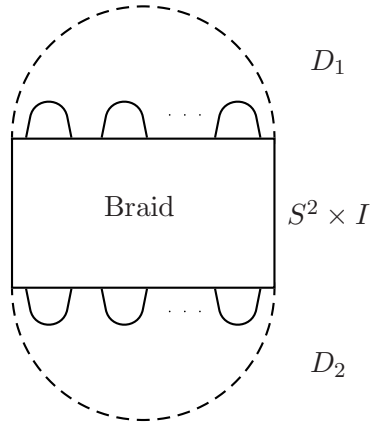


FIGURE 7. A plat diagram and the corresponding splitting of S^3

Now D_1 (respectively D_2) is covered by a handlebody H_1 (respectively H_2) whose genus depends only on the number of caps (respectively cups), see [2]. Since there are as many caps as cups the two handlebodies have the same genus. On the other hand $S^2 \times I$ is covered by a “thick” surface “realizing” a homeomorphism $f : \partial H_1 \rightarrow \partial H_2$. Therefore one gets a Heegaard splitting of the total space of the covering represented by the colored link.

Definition 1.3.6. A *normalized diagram* is a colored link diagram in a plat form such that its top and bottom are equal to

$$\rho_{\text{stand}} := \overset{12}{\frown} \quad \overset{14}{\frown} \quad \dots \quad \overset{1m}{\frown} \quad \overset{23}{\frown} \quad \dots \quad \overset{23}{\frown}$$

Remark 1.3.7. A variety of different normalizations can be found in the literature. The one chosen above is most suitable for the purposes of this work.

Proposition 1.3.8. *Every colored link has a normalized diagram.*

The following combinatorial lemma will be used in the proof.

Lemma 1.3.9 (Bernstein-Edmonds). *Let $\rho = \sigma_0, \sigma_1, \dots, \sigma_{2k-2}, \sigma_{2k}$ be a sequence of transpositions of \mathcal{S}_m satisfying the following four conditions:*

- (i) $\sigma_0\sigma_1 \cdots \sigma_{2k-1} = id$
- (ii) each σ_i is a transposition
- (iii) the subgroup of \mathcal{S}_m generated by the σ_i 's is transitive
- (iv) $\sigma_{2j} = \sigma_{2j+1}$ for $j = 0, \dots, k-1$.

Then ρ can be related to any other such sequence via a finite sequence of the following two moves:

- (a) interchange the position of any two pairs
- (b) replace a pair of transpositions by its conjugate by a neighboring pair.

Proof. Proposition 3.8 of [2] □

Proof of 1.3.8. It suffices to show that moves (a) and (b) of Lemma 1.3.9 can be realized by colored isotopy. This is done in Figure 8 □

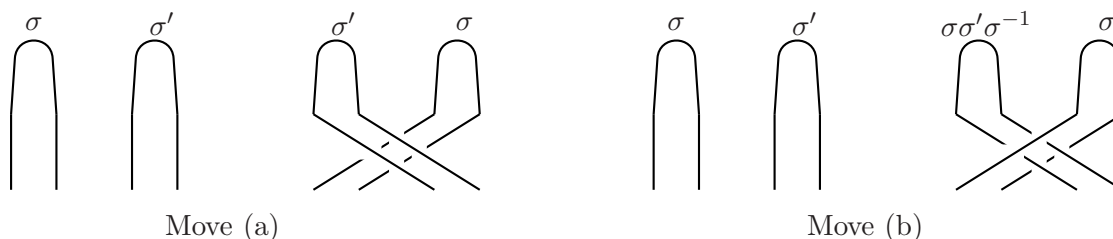


FIGURE 8. Realizing moves (a) and (b)

1.4. **Dimming the lights.** There is an exact sequence of groups:

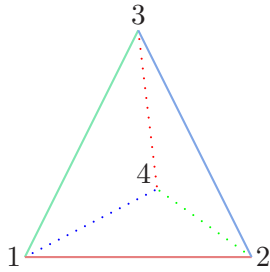
$$1 \longrightarrow V \longrightarrow \mathcal{S}_4 \xrightarrow{\kappa} \mathcal{S}_3 \longrightarrow 1$$

where $V = \{id, (12)(34), (14)(23), (13)(24)\}$ is Klein's Vierergruppe. For the purposes of this work κ is best seen by identifying the edges of a numbered tetrahedron with the transpositions of \mathcal{S}_4 and the edges of its front face with the transpositions of \mathcal{S}_3 (see Figure 9). Then κ fixes the front edges and sends each back edge to its opposite edge.

It is customary to identify, see [11] for example, the three transpositions of \mathcal{S}_3 with three colors Red, Green and Blue via $R = (12)$, $B = (23)$ and $G = (13)$. The above exact sequence then suggests the identification of the transpositions of \mathcal{S}_4 with three colors that come in light and dark shades. Denoting by \tilde{X} the dark shade of a color X this identification is given explicitly by:

$$\begin{aligned} R &= (12) & B &= (23) & G &= (13) \\ \tilde{R} &= (24) & \tilde{B} &= (14) & \tilde{G} &= (24) \end{aligned}$$

The homomorphism κ can then be described as “dimming the lights” so that the two shades of the same color cannot be distinguished.

FIGURE 9. How to see the map κ

There is an induced functor from the category of “bi-tricolored” braids to the category of tricolored braids which will also be referred to as dimming the lights. Dimming the lights obviously commutes with the lifting functor.

1.5. Adding a trivial sheet. Let $p : M \longrightarrow S^n$ be an m -sheeted covering over the n -sphere branched over the codimension-2 submanifold L . One can construct an $m + 1$ -sheeted covering of S^n with the same total space and branched over $L \sqcup K$, where K is an unknotted $n - 2$ -sphere contained in a ball which is disjoint from L , as follows:

Let D be an $(n - 1)$ -disk disjoint from L with $\partial D = K$. Since D is simply connected, $p^{-1}(D)$ consists of m disjoint $(n - 1)$ -disks each mapping homeomorphically onto D . Choose one of these disks, say \tilde{D} , and cut M open along \tilde{D} , to get a manifold M_{cut} together with a projection $p_{\text{cut}} : M_{\text{cut}} \longrightarrow S^n$. The boundary of M_{cut} is obtained by gluing two copies \tilde{D}_1 and \tilde{D}_2 of \tilde{D} along their boundary and is therefore homeomorphic to S^{n-1} .

Also cut a copy of S^n , the $(m + 1)^{\text{th}}$ sheet, open along K to get an n -disk S_{cut} with its boundary obtained by gluing two copies D_1 and D_2 of D along their boundary.

Now glue M_{cut} and S_{cut} along their boundary in such a way that \tilde{D}_1 is glued to D_2 and \tilde{D}_2 is glued to D_1 , to get a connected sum of M with S^n which is homeomorphic to M . By gluing p_{cut} and the gluing map $S_{\text{cut}} \longrightarrow S^n$ one gets a projection

$$p' : M \longrightarrow S^n.$$

It is easily checked that $p' : M \longrightarrow S^n$ is an $(m + 1)$ -sheeted covering branched over $L \sqcup K$. p' is said to be obtained by p by *adding a trivial sheet*. $\pi_1(S^n \setminus L \sqcup K)$ is a free product of $\pi_1(S^n \setminus L)$ and an infinite cyclic group generated by a meridian around K and it is clear that the monodromy of p' coincides with the monodromy of p in the first factor and associates a transposition of the form $(i, m + 1)$ to the meridian around K . Therefore p' is simple whenever p is.

2. THE 3-SHEETED CASE

In this section we give some results when the degree of the coverings is 3. These results will be used either directly or by analogy in the study of coverings of degree 4.

2.1. 3-sheeted Coverings of S^2 . Although we are mainly interested in 3-sheeted coverings of the 2-sphere S^2 it is convenient to consider more generally coverings of the 2-disc D^2 . Recall from Section 1.2 how such coverings are represented as finite sequences of

transpositions of \mathcal{S}_3 : the length of the sequence is the number of branch values and the i^{th} term of the sequence is the i^{th} monodromy.

Consider the following covering over D^2

$$\rho(n) := (12), (12), (23), (23), \dots, (23) \quad ,$$

where there are n branch values and all non displayed monodromies are equal to (23) . $\rho(n)$ corresponds to a covering over S^2 iff n is even (see Section 1.2 on page 4). In that case the Riemann-Hurwitz formula (1.2.2) gives the following relation between the number of branch values n and the genus g of the total space:

$$n = 2g - 4 \quad .$$

Denote by $L(n)$ the subgroup of the braid group B_n that fixes $\rho(n)$. Recall from that section 1.2 on page 7, that $L(n)$ (denoted $\text{Aut}(\rho(n))$ there) coincides with the subgroup of the mapping class group $\mathfrak{M}_{0,1,n}$ that consists of liftable (isotopy classes of) homeomorphisms.

This covering was studied by Birman and Wajnryb in [4]. The remaining of this section is an exposition of the results of that paper that are relevant to this study.

Theorem 2.1.1 (Birman-Wajnryb). *$L(n)$ is the smallest subgroup of B_n containing the following elements:*

$$\beta_0, \beta_1^3, \beta_2, \beta_3, \dots, \beta_{n-2}, \quad \text{and if } n \geq 6, \quad \delta_4$$

where $\delta_4 = [\beta_4]\beta_3\beta_2\beta_1^2\beta_2\beta_3^2\beta_2\beta_1$ is the rotation around the interval d_4 shown in Figure 10.

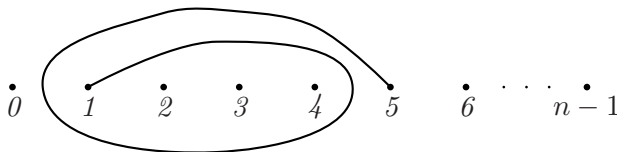


FIGURE 10. The interval d_4

Proof. Theorem 6.1 of [4]. See also Theorem 3.1 of the same paper. Note that the same symbol is used there to denote an interval and the rotation around it. \square

From now on the generators given in the above theorem will be referred to as *the* generators of $L(n)$. Observe that each generator is a power of a rotation around some interval. Therefore according to Lemma 1.2.2 their lifts can be determined by determining how these intervals lift. One gets the following theorem, where the notation used for elements of the mapping class group $\mathfrak{M}(E(\rho(n)))$ is that of [16] (see Appendix A).

Theorem 2.1.2 (Birman-Wajnryb). *The lifting homomorphism $\lambda : L(n) \longrightarrow \mathfrak{M}(E(\rho(n)))$ is given on the generators of $L(n)$ by*

$$(2.1.1) \quad \lambda(x) = \begin{cases} id & \text{if } x = \beta_0 \text{ or } \beta_1^3 \\ a_i & \text{if } x = \beta_{2i} \text{ with } i \geq 1 \\ b_i & \text{if } x = \beta_{2i+1} \text{ with } i \geq 1 \\ d & \text{if } x = \delta_4 \end{cases}$$

Proof. Figure 11 gives an explicit model of $\rho(n)$. This model is constructed by cutting and pasting as described in Section 1.2, page 6. The 2-sphere is cut open along the intervals $x_0, x_2, \dots, x_{2g-2}$. Since the monodromy along a loop that goes around one of those intervals is id the resulting $g - 1$ -holed sphere lifts to three disjoint copies of itself. The cuts are shown in blue and its assumed in Figure 11 that free blue loops are “sewn” to become intervals so that we get a closed surface covering S^2 . d_4 and how it lifts to an arc and a loop isotopic to d is shown in red. The check for the other generators is rather trivial. \square

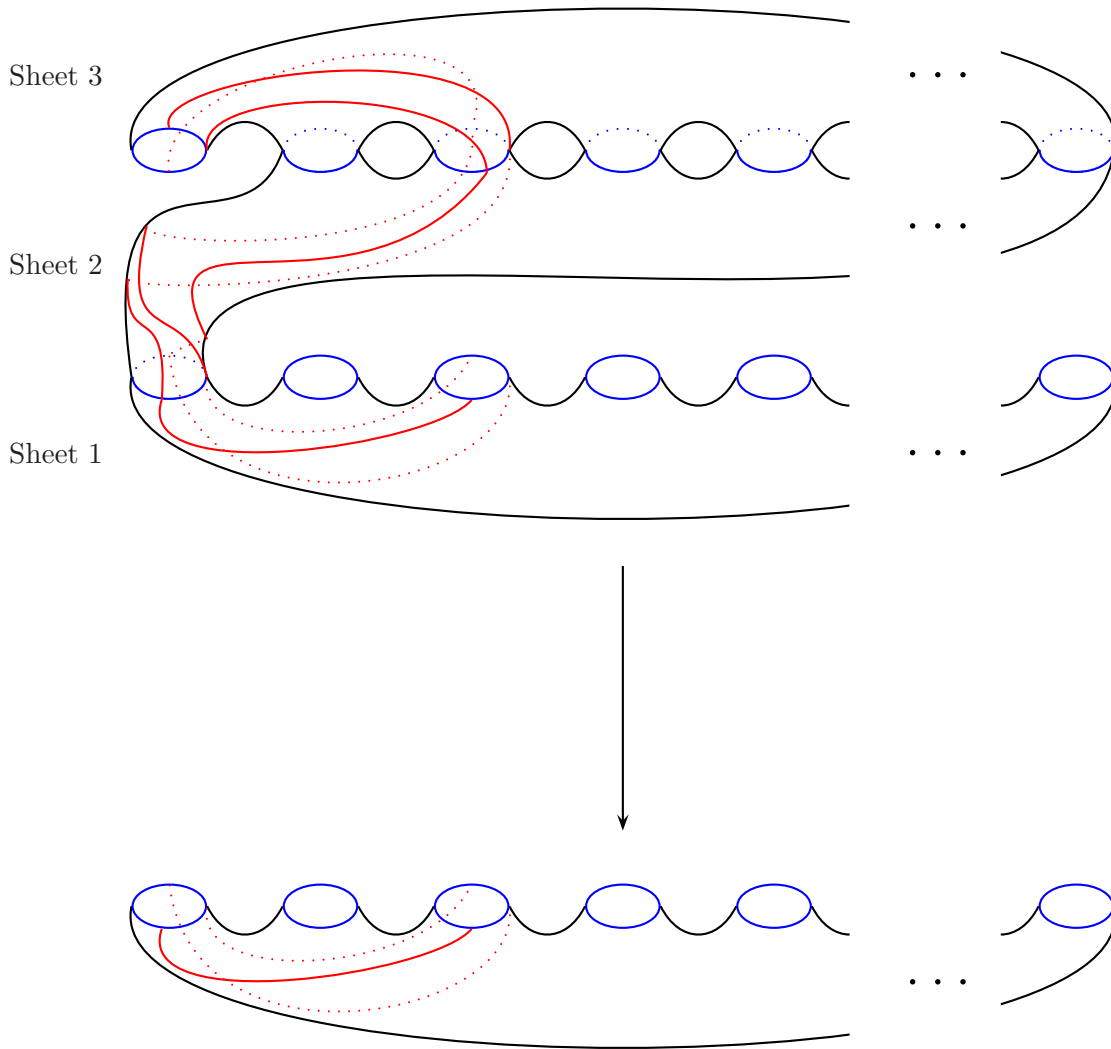


FIGURE 11. The covering $\rho(n)$ and how d_4 lifts

As an immediate corollary one gets the following:

Theorem 2.1.3. *For 3-sheeted coverings of the 2-sphere the lifting homomorphism is surjective.*

Proof. All Wajnryb generators are in the image of the lifting homomorphism. \square

Furthermore using Wajnryb's presentation the authors of [4] gave a set of normal generators of the kernel of the lifting homomorphism:

Theorem 2.1.4 (Birman-Wajnryb). *The kernel of the lifting homomorphism $\lambda : L(n) \longrightarrow \mathfrak{M}(E(\rho(n)))$ is the smallest normal subgroup of $L(n)$ containing the following elements (recall that $[\beta']\beta$ for braids β', β means $\beta^{-1}\beta'\beta$): β_0, β_1^3, B and D , where*

$$B = (\beta_2\beta_3\beta_4)^4([\delta_4^{-1}]\beta_4^{-1}\beta_3^{-1}\beta_2^{-2}\beta_3^{-1}\beta_4^{-1}\beta_5^{-1})\delta_4^{-1},$$

$$D = \beta_{2g+2}\chi\beta_{2g+2}^{-1}\chi^{-1},$$

Where:

$$\chi = \beta_{2g+1}\beta_{2g} \cdots \beta_3\beta_2^2\beta_3 \cdots \beta_{2g}\beta_{2g+1},$$

Proof. See the proof of Theorems 5.1 and 6.1 of [4]. See also the Errata [5]. \square

Remark 2.1.5. The normal generators in [4] are slightly different than the ones given above. In particular the element we denote by B is denoted by B' there while B denotes an element which is equal to B' modulo the other generators. The generators we use are the same as those in [11].

2.2. 3-sheeted Coverings of S^3 . Recall from Section 1.3 that coverings over S^3 are represented by colored link diagrams. In particular for 3-sheeted coverings we have *tricolored* link diagrams that is link diagrams whose arcs are colored with three colors (corresponding to the three transpositions of \mathfrak{S}_3) in such a way that

- a) at least two colors are used (to ensure that the total space of the covering is connected), and
- b) at each crossing there are either three colors or only one (to ensure that the Wirtinger relations are preserved).

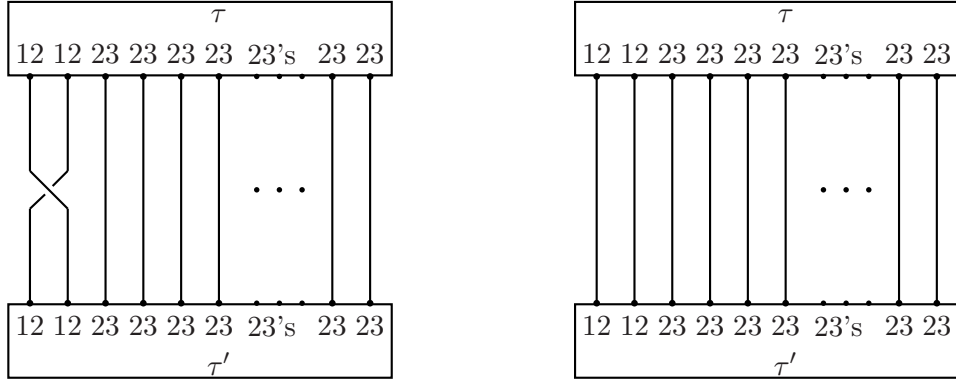
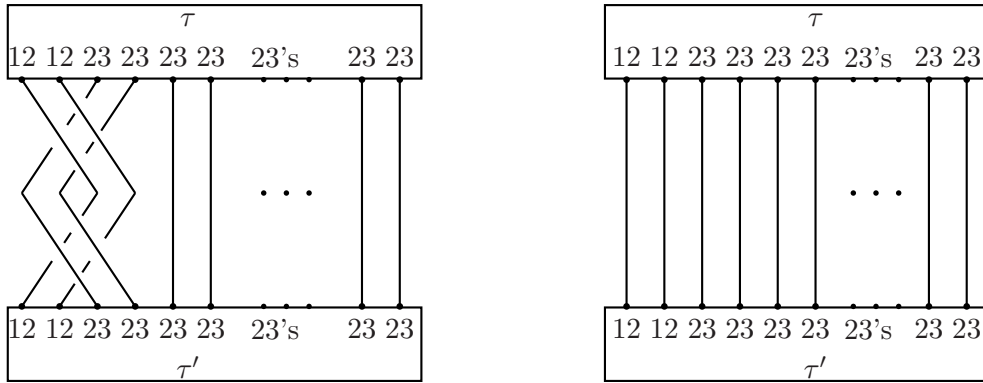
The following theorem was proved independently by Montesinos in [9] and Hilden in [8]. The proof we provide is essentially that of Hilden.

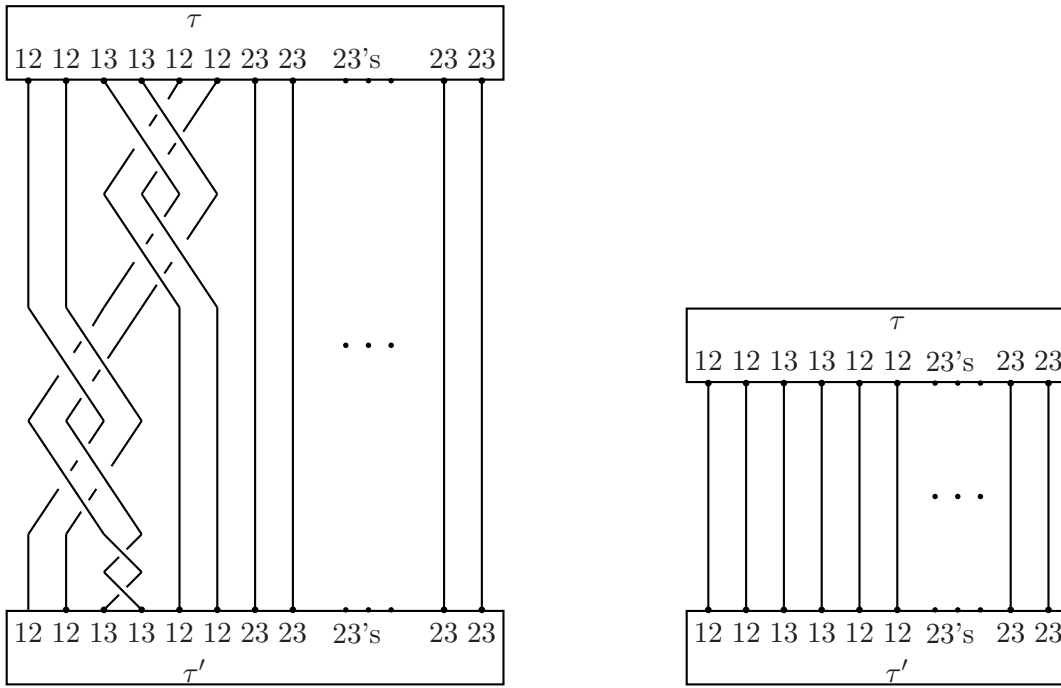
Theorem 2.2.1 (Hilden, Montesinos). *Every orientable closed 3-manifold is a simple 3-sheeted covering of the 3-sphere.*

Proof. Since by Theorem 2.1.3 the lifting homomorphism is surjective all Heegaard splittings can be realized (see Section 1.3). \square

Thus any orientable closed 3-manifold can be represented by a tricolored link diagram. Of course the same manifold manifests itself as a 3-sheeted covering of S^3 in many different ways and therefore admits several presentations as a tricolored link. Naturally then one asks the question whether there is a finite set of moves such that two tricolored link diagrams represent the same 3-manifold iff they can be related via a finite sequence of moves from this set. For some time it was conjectured that the "Montesinos move" \mathcal{M} shown in Figure 5 is the answer. However Montesinos gave a counterexample in [10]. Then in the 90's Piergallini proved the following theorem in [11].

Theorem 2.2.2 (Piergallini). *Two tricolored link diagrams represent the same manifold iff they can be related (up to colored Reidemeister moves) by a finite sequence of moves of the types \mathcal{M} , P_{II} , P_{III} , P_{IV} described in Figures 5, 12, 13, 14 respectively.*

FIGURE 12. Move P_{II} FIGURE 13. Move P_{III}

FIGURE 14. Move P_{IV}

Proof. Move \mathcal{M} does not change the represented manifold since the braid on its left side lifts to identity. That the moves II, III, and IV do not change the represented manifold follows for example from the proof of Theorem 2.2.3 below where it is shown that they can be realized using moves \mathcal{M} , \mathcal{P} and addition/deletion of a trivial sheet. (There is no vicious circle here since this part of the theorem is not used in the proof of 2.2.3).

For the reverse implication we just give a sketch of the contents of [11]. Let D and D' be two tricolored links representing the same 3-manifold.

Convert D and D' to normalized diagrams (still denoted D and D'), see Section 1.3. This gives us two Heegaard diagrams of the same manifold which according to Appendix D are stably equivalent. The proof then proceeds as follows:

Step 1: Stabilization of Heegaard splittings can be realized at the level of normalized diagrams via isotopy.

Indeed performing the modification shown in Figure 15 the corresponding Heegaard splitting changes by a connected sum with the genus-1 splitting of S^3 .

Therefore by repeatedly applying the modification in Figure 15 one can change the diagrams D and D' so that they represent equivalent Heegaard splittings i.e. so that we

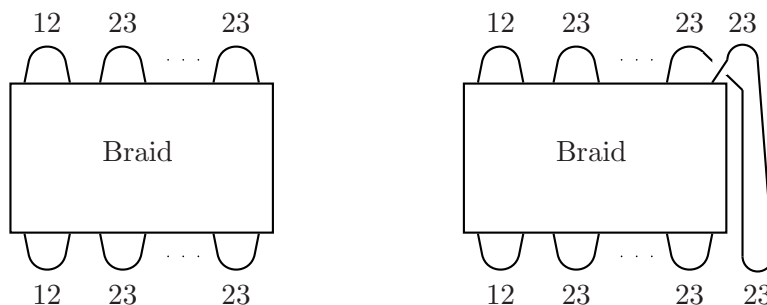


FIGURE 15. Heegaard Stabilization

have a commutative diagram:

$$\begin{array}{ccccc}
 H_1 & \supset & \partial H_1 & \xrightarrow{\phi} & \partial H_2 & \subset & H_2 \\
 \downarrow & & \downarrow f_1 & & \downarrow f_2 & & \downarrow \\
 H_1 & \supset & \partial H_1 & \xrightarrow{\phi'} & \partial H_2 & \subset & H_2
 \end{array}$$

where $M = H_1 \cup_{\phi} H_2$ and $M = H_1 \cup_{\phi'} H_2$ are the Heegaard splittings corresponding to the diagrams D and D' respectively, and the vertical maps are homeomorphisms. In particular the homeomorphisms f_1 and f_2 are homeomorphisms of surfaces that extend to homeomorphisms of the handlebodies.

Step 2: For any homeomorphism $\phi : \partial H_1 \rightarrow \partial H_1$ that extends to a homeomorphism $H_1 \rightarrow H_1$ there is a tricolored braid that lifts to ϕ and can be added at the top (or bottom) of a normalized diagram via isotopy and move \mathcal{M} .

This is done using the results of Suzuki in [15] where a finite set of generators for the group of isotopy classes of homeomorphisms of a surface that extend to homeomorphisms of the handlebody is given. Piergallini in Section 2 of [11] shows that each of these generators can be added at the top (and hence at the bottom) of a normalized diagram using isotopy and move \mathcal{M} .

Therefore, referring to the commutative diagram above, one can add a colored braid lifting to f_1 at the top, and a colored braid lifting to f_2^{-1} at the bottom of D' . The resulting diagram (still denoted D') induces the same Heegaard diagram as D that is, the braids of D and D' lift to the same homeomorphism of ∂H . So if β (resp. β') is the braid of D (resp. D') then

$$\exists \beta'' \in Ker(\lambda) \quad \beta = \beta' \beta''$$

where λ is the lifting homomorphism.

Step 3: Any braid in the kernel of the lifting homeomorphism can be added at the bottom of a normalized diagram using the moves \mathcal{M} , II, III and IV.

Piergallini shows that in Section 3 of [11] by showing that each of the normal generators in Theorem 2.1.4 can be added at the bottom of a normalized diagram.

Therefore the braid β'' of the above equation can be added at the bottom of D' to convert it to D . □

Notice the following difference between move \mathcal{M} and the other three moves: in order to check that moves P_{II} - P_{IV} can be applied one needs to know the structure of the whole link while for move \mathcal{M} one only needs to know a small part of the link. In this sense \mathcal{M} is a “local” move while the other three are not.

Recall from Section 1.5 the procedure of adding a trivial sheet to coverings over spheres. In the case of a 3-sheeted covering over S^3 it produces a 4-sheeted covering over S^3 with the same total space. In terms of colored diagrams we have the following move (Figure 16): to a tricolored link diagram D add an unknotted unlinked component colored by a dark color (see Section 1.4) to get a bi-tricolored link diagram. This move will be referred to as addition of a trivial sheet and its reverse move as deletion of a trivial sheet.

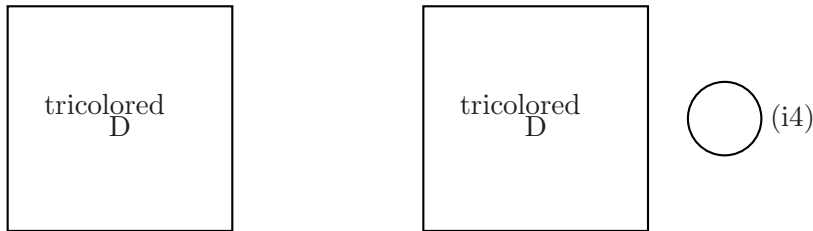


FIGURE 16. Adding a trivial sheet

After proving in [10] that \mathcal{M} is not enough Montesinos asked in the same paper whether moves \mathcal{M} , \mathcal{P} (see Figure 6) together with addition/deletion of a fourth trivial sheet suffice to relate any two tricolored link presentations of the same manifold. Piergallini gave a positive answer in [12]:

Theorem 2.2.3 (Piergallini). *Two tricolored link diagrams represent the same manifold iff they can be related using moves \mathcal{M} , \mathcal{P} and addition/deletion of a fourth trivial sheet (and of course colored Reidemeister moves).*

Proof. Piergallini proves in Theorem A of [12] that the moves II, III and IV can be realized using moves \mathcal{M} and \mathcal{P} after one adds a trivial sheet. □

3. FOUR SHEETS I: COVERINGS OVER S^2

In this section we establish for 4-sheeted coverings of S^2 results similar to the results of Section 2.1. Again it is more convenient to work with coverings over the disc and then restrict attention to coverings with boundary monodromy id, see Section 1.2, page 4. Specifically we consider the following 4-sheeted covering of the 2-disc:

$$\rho_{23}^n := (12), (12), (14), (14), (23), \dots, (23)$$

where there are n branch values and all the missing monodromies are equal to (23). (This notation is part of a more general notation, see Definition 3.1.1 below.) After dimming the lights (see Section 1.4) we get the 3-sheeted covering $\rho(n)$ of Section 2.1 and since dimming the lights commutes with lifting we get that

$$\text{Aut}(\rho_{23}^n) \subset L(n)$$

where $L(n)$ denotes $\text{Aut}(\rho(n))$ as in Section 2.1. Furthermore if $\beta \in L(n)$ then dimming the lights for $(\rho_{23}^n)\beta$ will again give $\rho(n)$. Thus we have an action of $L(n)$ on the set $\kappa^{-1}(\rho(n))$ of 4-sheeted coverings that give $\rho(n)$ after dimming the lights, and the isotropy group of ρ_{23}^n under this action is $\text{Aut}(\rho_{23}^n)$.

Using this action in Subsection 3.1 we construct a 2-dimensional cell complex whose fundamental group is the quotiented automorphism group $\overline{\text{Aut}}(\rho_{23}^n)$. The complex is then used in Subsection 3.2 to produce generators for this group. Finally in Subsection 3.3 we use these generators to find normal generators for the kernel of the (quotiented) lifting homeomorphism.

3.1. The Complex. Recall that κ denotes dimming the lights, $L = \{A_0, A_1, \dots, A_{n-1}\}$ denotes the set of branched values and that α_i for $i = 0, 1, \dots, n-1$ denotes the generator of $\pi_1(D^2 \setminus L)$ that is represented by a lasso going around A_i .

Definition 3.1.1. Let

$$\mathcal{C}^n := \{\rho \in \kappa^{-1}(\rho(n)) \mid \rho(\alpha_0) = \rho(\alpha_1) = (12)\}$$

For $I \subseteq \{2, 3, \dots, n-1\}$ define the 4-sheeted coverings $\rho_I^n, \tilde{\rho}_I^n$ of D^2 via:

$$\rho_I^n(\alpha_i) := \begin{cases} (12) & \text{if } i = 0, 1 \\ (14) & \text{if } i \in I \\ (23) & \text{if } i \notin I \end{cases}, \quad \tilde{\rho}_I^n(\alpha_i) = \begin{cases} (12) & \text{if } i = 0, 1 \\ (23) & \text{if } i \in I \\ (14) & \text{if } i \notin I \end{cases}$$

Recall the generators of $L(n)$ given in Theorem 2.1.1. The following lemma describes how δ_4 acts on

$$\mathcal{C}^6 = \{\rho_\emptyset^6, \tilde{\rho}_\emptyset^6, \rho_{ij}^6, \tilde{\rho}_{ij}^6, \rho_i^6, \tilde{\rho}_i^6 \mid i, j = 2, 3, 4, 5\}.$$

Since $(\alpha_i)\delta_4 = \alpha_i$ for $i \geq 6$ this determines how δ_4 acts on elements of \mathcal{C}^n . The action of the remaining generators is clear.

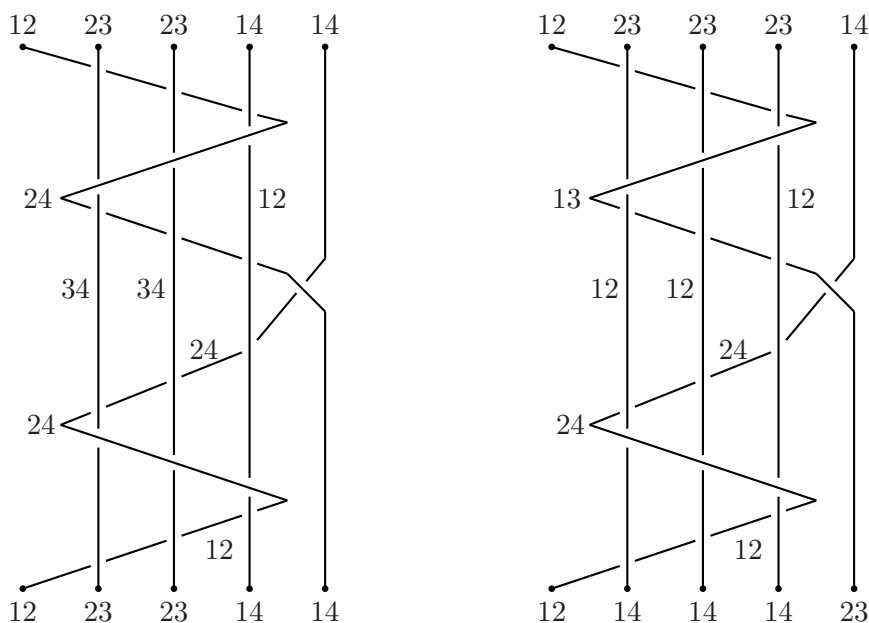
Lemma 3.1.2. δ_4 acts on \mathcal{C}^6 as follows: it fixes $\rho_\emptyset, \tilde{\rho}_\emptyset, \rho_{ij}$ and $\tilde{\rho}_{ij}$, while $(\rho_i)\delta_4 = \tilde{\rho}_i$.

Proof. Since $\delta_4 \in L(n)$ it fixes $\rho_\emptyset, \tilde{\rho}_\emptyset$. For the remaining cases see Figure 17.

Notice that these two cases are enough since δ_4 commutes with β_2, β_3 and, of course, with conjugations in the range. Furthermore by Lemma 3.1.8 it commutes with β_4 modulo the move \mathcal{M} . \square

Corollary 3.1.3. The action of $L(n)$ on $\kappa^{-1}(\rho(n))$ restricts to an action on \mathcal{C}^n .

Proof. We have to check that each of the generators of $L(n)$ preserves $\mathcal{C}(n)$, that is if the first two monodromies of a covering ρ are equal to (12) then the first two monodromies of $(\rho)\beta$ are also equal to (12), for $\beta \in L(n)$. Lemma 3.1.2 proves this for δ_4 , for the other generators it is obvious. \square

FIGURE 17. How δ_4 acts

Recall from page 8 that for a covering ρ , $N(\rho)$ denotes the normal subgroup of $\text{Aut}(\rho)$ “generated” by the moves \mathcal{M} and \mathcal{P} and that the quotient of $\text{Aut}(\rho)$ by that subgroup is denoted by $\overline{\text{Aut}}(\rho)$.

A standard technique for understanding a group is to realize it as the fundamental group of some 2-complex. We construct such a complex for the quotiented automorphism group:

Definition 3.1.4. Given $\rho \in \kappa^{-1}(\rho(n))$ define a 2-complex $\mathcal{C}(\rho)$ as follows:

- The 0-cells of $\mathcal{C}(\rho)$ are the points of the $L(n)$ -orbit of ρ .
- The 1-cells of $\mathcal{C}(\rho)$ are labelled by the generators of $L(n)$. There is one 1-cell labelled by β for each *unordered* pair $\{\rho', \rho''\} \subseteq \kappa^{-1}(\rho(n))$ with the property $\rho'\beta = \rho''$.
- A path on the 1-skeleton gives a word on the generators of $L(n)$. There is a 2-cell attached along each closed path whose word lies in $N(\rho')$ for some ρ' in the path.

Notice that each generator of $L(n)$ acts as an involution and therefore we don’t need to orient the 1-dimensional cells. Clearly $\pi_1(\mathcal{C}(\rho), \rho) = \overline{\text{Aut}}(\rho)$. Also notice that one can get a complex whose fundamental group is $\text{Aut}(\rho)$ by attaching only the 2-cells that kill the words that are equal to identity in $L(n)$.

The complex $\mathcal{C}(\rho)$ will be confused with its 0-skeleton when the confusion is easily resolved.

Terminology: A vertex is a 0-cell. An edge is a 1-cell with its boundary points attached to distinct vertices. A loop is a 1-cell with its boundary points attached to the same vertex.

Lemma 3.1.5. *At the level of 0-skeletons:*

- (a) $\mathcal{C}(\rho_{23}^n)$ consists of those coverings which:
- start with (12), (12),
 - have at least one monodromy equal to (14), and at least one monodromy equal to (23),
 - have an even number of monodromies equal to (14).
- (b) $\mathcal{C}(\tilde{\rho}_{23}^n)$ consists of those coverings which:
- start with (12), (12),
 - have at least one monodromy equal to (14), and at least one monodromy equal to (23),
 - have an even number of monodromies equal to (23).
- (c) For n even, $\mathcal{C}(\rho_2^n)$ consists of those coverings which:
- start with (12), (12),
 - have at least one monodromy equal to (14), and at least one monodromy equal to (23),
 - have an odd number of monodromies equal to (14).

Proof. Let $\mathcal{C}_{\text{id}}^n$ (resp. $\mathcal{C}_{(23)}^n$) be the set of coverings with the properties described in (a) and n even (resp. odd). Clearly $\rho_{23}^n \in \mathcal{C}_{\text{id}}^n$ (resp. $\mathcal{C}_{(23)}^n$) and $L(n)$ preserves $\mathcal{C}_{\text{id}}^n$ (resp. $\mathcal{C}_{(23)}^n$).

This is obvious for $\beta_0, \beta_1^3, \beta_2, \dots, \beta_{n-2}$ and 3.1.2 proves it for δ_4 .

To see that every covering in $\mathcal{C}_{\text{id}}^n$ (resp. $\mathcal{C}_{(23)}^n$) is in the $L(n)$ -orbit of ρ_{23}^n , observe that $\langle \beta_2, \dots, \beta_{n-2} \rangle$ acts transitively on the subset of $\mathcal{C}_{\text{id}}^n$ (resp. $\mathcal{C}_{(23)}^n$) consisting of coverings with any fixed even number of monodromies equal to (14), while δ_4 , acting on suitably chosen coverings, increases or decreases the number of monodromies equal to (14) by 2.

(b) and (c) are proved similarly by (defining and) looking at $\mathcal{C}_{(14)}^n$ and $\mathcal{C}_{(14)(23)}^n$. \square

Proposition 3.1.6. \mathcal{C}_{\bullet}^n (defined in the proof of Lemma 3.1.5) consists of those coverings of \mathcal{C}^n that have connected total space and boundary monodromy equal to \bullet .

Proof. Obvious. \square

Conjugation by (12)(34) (i.e interchanging the dark and light shades of Blue) defines an involution \sim on \mathcal{C}^n . Clearly \sim interchanges $\mathcal{C}_{(23)}^n$ and $\mathcal{C}_{(14)}^n$ and preserves $\mathcal{C}_{\text{id}}^n$ and $\mathcal{C}_{(14)(23)}^n$. In particular $\mathcal{C}_{(23)}^n$ and $\mathcal{C}_{(14)}^n$ are isomorphic.

Now given a covering with n branch values one can “add” one more point with prescribed monodromy at the end to get a covering with $n+1$ branch values. More formally, for each n there are two embeddings:

$$i_{(23)}^n : \mathcal{C}^n \longrightarrow \mathcal{C}^{n+1},$$

and

$$i_{(14)}^n : \mathcal{C}^n \longrightarrow \mathcal{C}^{n+1}$$

which are obviously $L(n)$ -equivariant if B_n is (as usual) considered to be the subgroup of B_{n+1} that “doesn’t touch” the last string.

Proposition 3.1.7. For even n :

a) At the level of 0 skeletons:

$$\mathcal{C}_{\text{id}}^n = i_{(23)}^{n-1}(\mathcal{C}_{(23)}^{n-1}) \sqcup i_{(14)}^{n-1}(\mathcal{C}_{(14)}^{n-1}),$$

and each vertex of $i_{(23)}i_{(14)}(\mathbb{C}_{(14)(23)}^{n-2})$ is joined by an edge labelled by β_{n-2} to the corresponding vertex of $i_{(14)}i_{(23)}(\mathbb{C}_{(14)(23)}^{n-2})$. These are the only new edges.

b) At the level of 0-skeletons:

$$\mathbb{C}_{(14)(23)}^n = i_{(23)}^{n-1}(\mathbb{C}_{(14)}^{n-1}) \sqcup i_{(14)}^{n-1}(\mathbb{C}_{(23)}^{n-1})$$

and each vertex of $i_{(23)}i_{(14)}(\mathbb{C}_{id}^{n-2} \sqcup \{\rho_\emptyset^{n-2}\} \sqcup \{\tilde{\rho}_\emptyset^{n-2}\})$ is joined by an edge labelled by β_{n-2} to the corresponding vertex of $i_{(14)}i_{(23)}(\mathbb{C}_{id}^{n-2} \sqcup \{\rho_\emptyset^{n-2}\} \sqcup \{\tilde{\rho}_\emptyset^{n-2}\})$. These are the only new edges.

For odd n :

At the level of 0 skeletons:

$$\mathbb{C}_{(23)}^n = i_{(23)}^{n-1}(\mathbb{C}_{id}^{n-1} \sqcup \{\tilde{\rho}_\emptyset^{n-1}\}) \sqcup i_{(14)}^{n-1}(\mathbb{C}_{(14)(23)}^{n-1}),$$

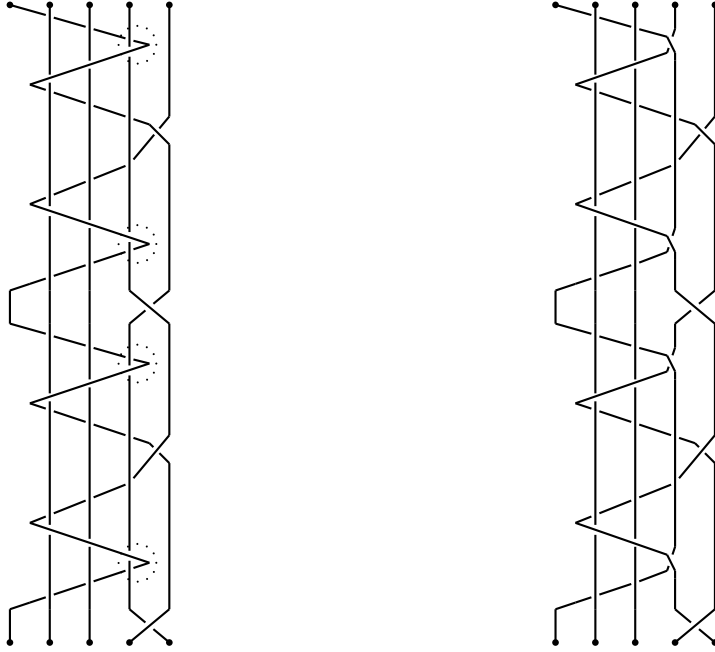
and each vertex of $i_{(23)}i_{(14)}(\mathbb{C}_{(14)}^{n-2} \sqcup \{\rho_\emptyset^{n-2}\})$ is joined by an edge labelled by β_{n-2} to the corresponding vertex of $i_{(14)}i_{(23)}(\mathbb{C}_{id}^{n-2} \sqcup \{\tilde{\rho}_\emptyset^{n-2}\})$. These are the only new edges.

Proof. Erase the last two points. □

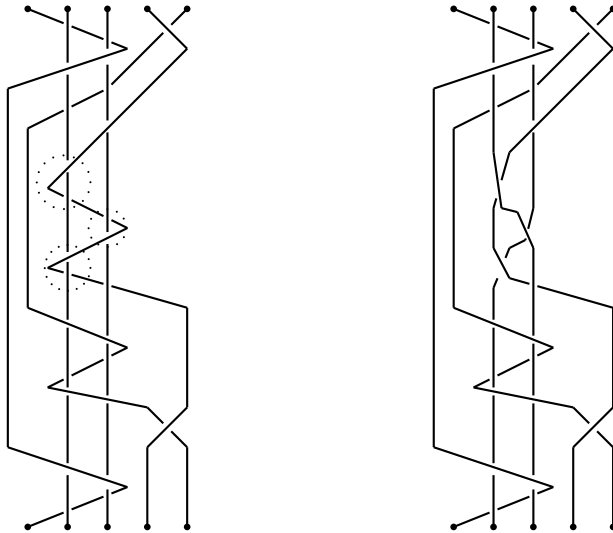
Lemma 3.1.8. β_4 commutes with δ_4 modulo the Montesinos move.

Proof. It suffices to show that $\delta_4\beta_4\delta_4^{-1}\beta_4^{-1} \equiv \text{id} \pmod{\mathcal{M}}$. This is done in the following pictures. The top of the braid is assumed colored by $\rho(n)$. The colors of the arcs are not shown as they can be easily deduced.

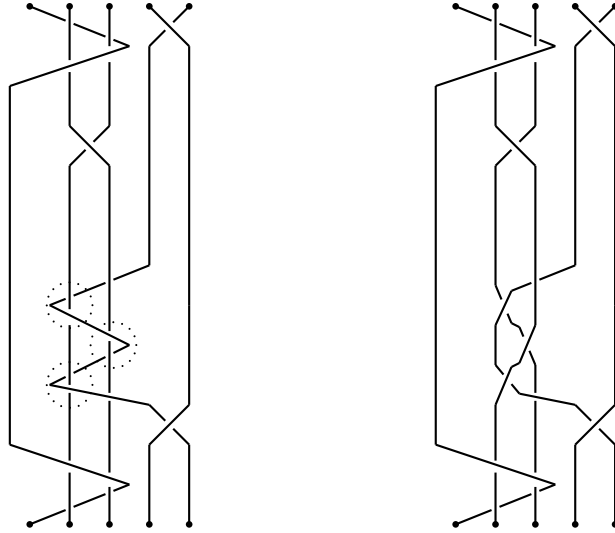
Start with $\delta_4\beta_4\delta_4^{-1}\beta_4^{-1}$ and perform \mathcal{M} inside the dotted circles:



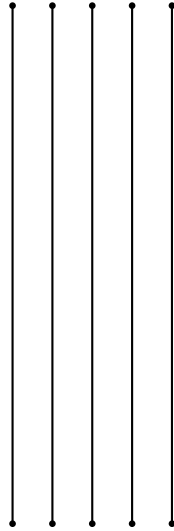
then isotope and perform \mathcal{M} moves inside the dotted circles:



Isotope and perform \mathcal{M} moves:



And finally isotope to get id:



□

Proposition 3.1.9. *Every square of the form*

$$\begin{array}{ccc} \rho_1 & \xrightarrow{y} & \rho_2 \\ x \downarrow & & \downarrow x \\ \rho_3 & \xrightarrow{y} & \rho_4 \end{array}$$

in $\mathcal{C}(\rho)$ bounds a 2-cell.

Proof. Assume first that $x, y \neq \delta_4$. Then it suffices to prove that x and y cannot be adjacent elementary braids. Suppose then, without loss of generality, that $x = \beta_i$ and $y = \beta_{i+1}$ for some $i \geq 2$. Since ρ_1 is moved by β_i its i^{th} and $(i+1)^{\text{th}}$ monodromies are different, and similarly its $(i+1)^{\text{th}}$ and $(i+2)^{\text{th}}$ monodromies are different. Thus without loss of generality

$$\rho_1 = \dots, \underset{i}{(14)}, \underset{i+1}{(23)}, \underset{i+2}{(14)} \dots$$

but then

$$\begin{aligned} \rho_1 \beta_i \beta_{i+1} &= \dots, \underset{i}{(23)}, \underset{i+1}{(14)}, \underset{i+2}{(14)} \dots \\ &\neq \dots, \underset{i}{(14)}, \underset{i+1}{(14)}, \underset{i+2}{(23)} \dots \\ &= \rho_1 \beta_{i+1} \beta_i \end{aligned}$$

a contradiction.

If one of the x, y is equal to δ_4 , say $x = \delta_4$, one only needs to check the cases $y = \beta_4$ and $y = \beta_5$ since d_4 doesn't meet any other "generating" interval.

If $y = \beta_4$, apply Lemma 3.1.8.

Since ρ_1 is moved by δ_4 it has either three monodromies equal to (14) and one equal to (23) or three monodromies equal to (23) and one equal to (14), in the spots 2, 3, 4, 5 and if $y = \beta_5$ then the 5th and 6th monodromies of ρ_1 are different. But then applying β_5 to ρ_1 one sees that ρ_2 has an even number of monodromies equal to (14) in the spots 2, 3, 4, 5 and it is therefore fixed by δ_4 , a contradiction. \square

3.2. Generators. We use the same symbol to denote an element of $\text{Aut}(\rho)$ and its image in $\overline{\text{Aut}}(\rho)$. This subsection is devoted to the proof of the following theorem:

Theorem 3.2.1. *For all even $n \geq 6$, $\overline{\text{Aut}}(\rho_{23}^n)$ is generated by $\beta_0, \beta_2, \beta_4, \beta_5, \dots, \beta_{n-2}, \delta_4$ and, if $n \geq 8$, δ_6 , where,*

$$\delta_6 = [\delta_4] \beta_5^{-1} \beta_4^{-1} \beta_3^{-1} \beta_2^{-1} \beta_6^{-1} \beta_5^{-1} \beta_4^{-1} \beta_3^{-1}.$$

Actually the following stronger statement will be proved:

Theorem 3.2.2. (a) *For each $n \geq 6$, $\overline{\text{Aut}}(\rho_{23}^n)$ is generated by $\beta_0, \beta_2, \beta_4, \beta_5, \dots, \beta_{n-2}, \delta_4$ and, if $n \geq 8$, δ_6 .*

(b) *For each even $n \geq 6$, $\overline{\text{Aut}}(\rho_{2,3,n-1}^n)$ is generated by $\beta_0, \beta_2, \beta_4, \dots, \beta_{n-3}, [\beta_{n-2}] \beta_{n-3}^{-1} \cdots \beta_3^{-1}$ and if $n \geq 8$, δ_4 and, if $n \geq 10$, δ_6 .*

The proof will be by induction on n . In the $n = 6$ case is not difficult to actually give generators for the automorphism group:

- Proposition 3.2.3.** (a) $\text{Aut}(\rho_{23}^6)$ is the smallest subgroup of B_6 containing the following elements: $\beta_0, \beta_1^3, \beta_2, \beta_3^2, \beta_4, \delta_4, [\beta_1^3]\beta_2^{-1}\beta_3^{-1}, [\delta_4]\beta_4^{-1}\beta_3^{-1}, [\beta_2^2]\beta_3^{-1}, [\beta_4^2]\beta_3^{-1}, [\beta_3^2]\beta_2^{-1}\beta_4^{-1}\beta_3^{-1}$
- (b) $\text{Aut}(\tilde{\rho}_4^6)$ is the smallest subgroup of B_6 containing the following elements: $\beta_0, \beta_1^3, \beta_2, \beta_3^2, \beta_4, \delta_4^2, [\beta_2^2]\beta_3^{-1}, [\delta_4^2]\beta_4^{-1}, \beta_4\delta_4\beta_4\delta_4^{-1}, [\beta_1^3]\beta_2^{-1}\beta_3^{-1}, \delta_4\beta_4\delta_4^{-1}\beta_4^{-1}, [\delta_4\beta_4\delta_4^{-1}]\beta_3^{-1}, [\beta_3]\beta_4^{-1}, [\beta_4]\beta_3^{-1}$.

Proof. (a) The graph in Figure 18 describes (the 1-skeleton of) $\mathcal{C}(\rho_{23}^6)$, together with a Schreier transversal drawn with wavy lines. Loops are not depicted as, for example, the presence of a loop labelled by β_1^3 at the vertex ρ_{23}^6 can be deduced by the absence of an edge labelled by β_1^3 at that vertex.

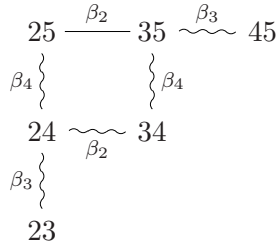


FIGURE 18. $\mathcal{C}(\rho_{23}^n)$ with a maximal tree

According to the Reidemeister-Schreier method (see for example [18]) $\text{Aut}(\rho_{23}^n)$ is generated by $g_i s_j \overline{g_i s_j}$ where g_i runs through the transversal, s_j runs through the generators and \bar{x} denotes the element of the transversal which ends at the endpoint of x . Then one gets the following generators:

$$g_i = \text{id}$$

$$\beta_0, \beta_1^3, \beta_2, \text{id}, \beta_4, \delta_4$$

$$g_i = \beta_3$$

$$\begin{aligned} &\beta_0, \beta_1^3, \\ &\beta_3 \beta_2 (\overline{\beta_3 \beta_2})^{-1} = \text{id}, \\ &\beta_3 \beta_3 (\overline{\beta_3 \beta_3})^{-1} = \beta_3^2, \\ &\beta_3 \beta_4 (\overline{\beta_3 \beta_4})^{-1} = \text{id}, \\ &\beta_3 \delta_4 (\overline{\beta_3 \delta_4})^{-1} = \beta_3 \delta_4 \beta_3^{-1} \\ &= \delta_4. \end{aligned}$$

$$g_i = \beta_3 \beta_4$$

$$\begin{aligned} &\beta_0, \beta_1^3, \\ &\beta_3 \beta_4 \beta_2 (\overline{\beta_3 \beta_4 \beta_2})^{-1} = \beta_3 \beta_4 \beta_2 \beta_4^{-1} \beta_2^{-1} \beta_3^{-1} \\ &= \text{id}, \\ &\beta_3 \beta_4 \beta_3 (\overline{\beta_3 \beta_4 \beta_3})^{-1} = \beta_3 \beta_4 \beta_3 \beta_4^{-1} \beta_3^{-1} \\ &= \beta_4, \\ &\beta_3 \beta_4 \beta_4 (\overline{\beta_3 \beta_4 \beta_4})^{-1} = \beta_3 \beta_4^2 \beta_3^{-1}, \\ &\beta_3 \beta_4 \delta_4 (\overline{\beta_3 \beta_4 \delta_4})^{-1} = \beta_3 \beta_4 \delta_4 \beta_4^{-1} \beta_3^{-1}. \end{aligned}$$

$$g_i = \beta_3\beta_2$$

$$\begin{aligned} &\beta_0, \\ &\beta_3\beta_2\beta_1^3(\overline{\beta_3\beta_2\beta_1^3})^{-1} = \beta_3\beta_2\beta_1^3\beta_2^{-1}\beta_3^{-1}, \\ &\beta_3\beta_2\beta_2(\overline{\beta_3\beta_2\beta_2})^{-1} = \beta_3\beta_2^2\beta_3^{-1}, \\ &\beta_3\beta_2\beta_3(\overline{\beta_3\beta_2\beta_3})^{-1} = \beta_2, \\ &\beta_3\beta_2\beta_4(\overline{\beta_3\beta_2\beta_4})^{-1} = \text{id}, \\ &\beta_3\beta_2\delta_4(\overline{\beta_3\beta_2\delta_4})^{-1} = \delta_4. \end{aligned}$$

$$g_i = \beta_3\beta_2\beta_4$$

$$\begin{aligned} &\beta_0, \\ &\beta_3\beta_2\beta_4\beta_1^3(\overline{\beta_3\beta_2\beta_4\beta_1^3})^{-1} = \beta_3\beta_2\beta_4\beta_1^3\beta_4^{-1}\beta_2^{-1}\beta_3^{-1} \\ &\quad = \beta_3\beta_2\beta_1^3\beta_2^{-1}\beta_3^{-1}, \\ &\beta_3\beta_2\beta_4\beta_2(\overline{\beta_3\beta_2\beta_4\beta_2})^{-1} = \beta_3\beta_2\beta_4\beta_2\beta_4^{-1}\beta_3^{-1} \\ &\quad = \beta_3\beta_2^2\beta_3^{-1}, \\ &\beta_3\beta_2\beta_4\beta_3(\overline{\beta_3\beta_2\beta_4\beta_3})^{-1} = \text{id}, \\ &\beta_3\beta_2\beta_4\beta_4(\overline{\beta_3\beta_2\beta_4\beta_4})^{-1} = \beta_3\beta_2\beta_4^2\beta_2^{-1}\beta_3^{-1} \\ &\quad = \beta_3\beta_4^2\beta_3^{-1}, \\ &\beta_3\beta_2\beta_4\delta_4(\overline{\beta_3\beta_2\beta_4\delta_4})^{-1} = \beta_3\beta_2\beta_4\delta_4\beta_4^{-1}\beta_2^{-1}\beta_3^{-1} \\ &\quad = \beta_3\beta_4\delta_4\beta_4^{-1}\beta_3^{-1}. \end{aligned}$$

$$g_i = \beta_3\beta_2\beta_4\beta_3$$

$$\begin{aligned} &\beta_0, \\ &\beta_3\beta_2\beta_4\beta_3\beta_1^3(\overline{\beta_3\beta_2\beta_4\beta_3\beta_1^3})^{-1} = \beta_3\beta_2\beta_4\beta_3\beta_1^3\beta_3^{-1}\beta_4^{-1}\beta_2^{-1}\beta_3^{-1} \\ &\quad = \beta_3\beta_2\beta_1^3\beta_2^{-1}\beta_3^{-1}, \\ &\beta_3\beta_2\beta_4\beta_3\beta_2(\overline{\beta_3\beta_2\beta_4\beta_3\beta_2})^{-1} = \beta_3\beta_2\beta_4\beta_3\beta_2\beta_3^{-1}\beta_4^{-1}\beta_2^{-1}\beta_3^{-1} \\ &\quad = \beta_3\beta_4\beta_2\beta_3\beta_2\beta_3^{-1}\beta_2^{-1}\beta_4^{-1}\beta_3^{-1} \\ &\quad = \beta_3\beta_4\beta_3\beta_4^{-1}\beta_3^{-1} \\ &\quad = \beta_4, \\ &\beta_3\beta_2\beta_4\beta_3\beta_3(\overline{\beta_3\beta_2\beta_4\beta_3\beta_3})^{-1} = \beta_3\beta_2\beta_4\beta_3^2\beta_4^{-1}\beta_2^{-1}\beta_3^{-1}, \\ &\beta_3\beta_2\beta_4\beta_3\beta_4(\overline{\beta_3\beta_2\beta_4\beta_3\beta_4})^{-1} = \beta_3\beta_2\beta_4\beta_3\beta_4\beta_3^{-1}\beta_4^{-1}\beta_2^{-1}\beta_3^{-1} \\ &\quad = \beta_3\beta_2\beta_3\beta_2^{-1}\beta_3^{-1} \\ &\quad = \beta_2, \\ &\beta_3\beta_2\beta_4\beta_3\delta_4(\overline{\beta_3\beta_2\beta_4\beta_3\delta_4})^{-1} = \beta_3\beta_2\beta_4\beta_3\delta_4\beta_3^{-1}\beta_4^{-1}\beta_2^{-1}\beta_3^{-1} \\ &\quad = \beta_3\beta_4\delta_4\beta_4^{-1}\beta_3^{-1}. \end{aligned}$$

(b) Similar calculations using the graph in Figure 19 which represents the 1-skeleton of $\mathcal{C}(\tilde{\rho}_4^6)$ together with a Schreier transversal give the result.

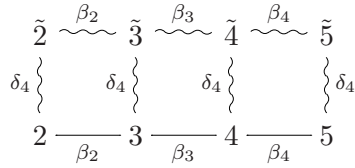


FIGURE 19. $\mathcal{C}(\tilde{\rho}_4^6)$ with a maximal tree

□

Corollary 3.2.4. (a) $\overline{\text{Aut}}(\rho_{23}^6)$ is generated by $\beta_0, \beta_2, \beta_4$ and δ_4 .

(b) $\overline{\text{Aut}}(\rho_2^6)$ is generated by β_0, β_3 and $[\beta_4]\beta_3^{-1}$.

Proof. One just needs to check that the generators given in Proposition 3.2.3 are equivalent $\text{mod } N$ to the generators given above. Given Lemma 3.1.8 the only slightly non trivial checks is to check that for any element of $\mathcal{C}(\rho_5^6)$ we have $\delta_4^2 \equiv \text{id} \pmod{N}$ and $[\beta_4]\beta_3^{-1} \equiv [\beta_3]\beta_4^{-1} \pmod{N}$. For the first look at Figure 20, where it is shown that $\delta_4 \equiv \delta_4^{-1} \pmod{N}$ for ρ_5^6 . For the second look at Figure 23 where a more general statement is shown. □

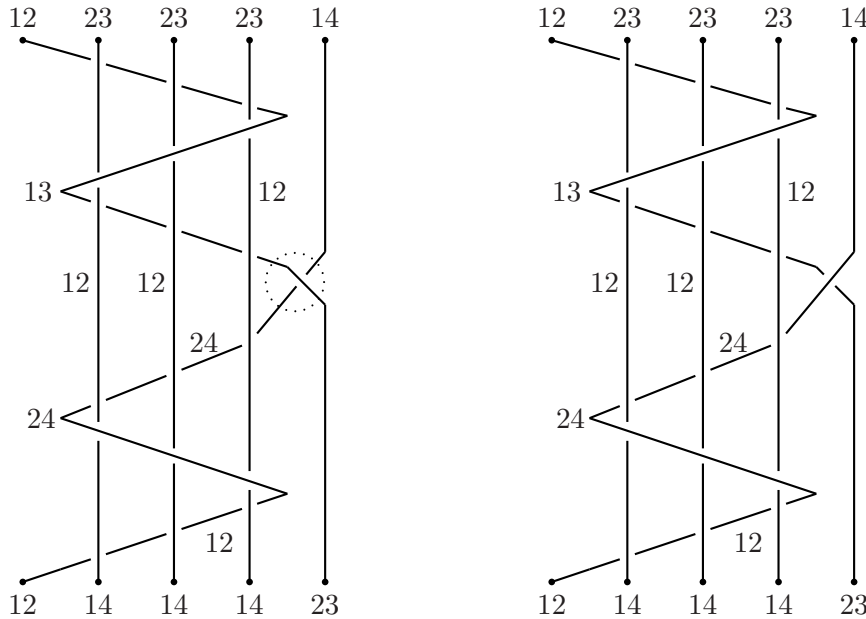


FIGURE 20. A \mathcal{P} move (inside the dotted circle) turns δ_4 into δ_4^{-1}

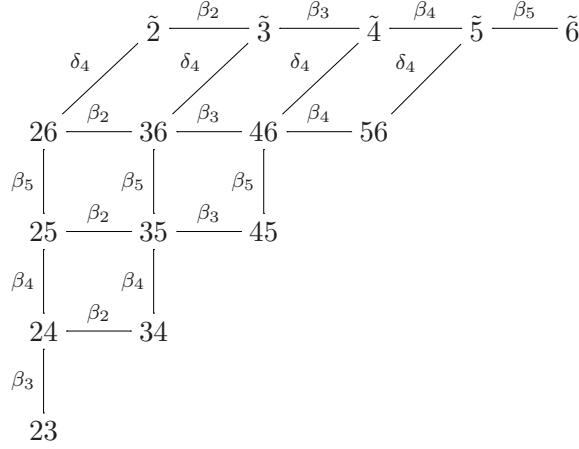
Next we do the $n = 7$ case. The 1-skeleton of $\mathcal{C}(\rho_{23}^7)$ is shown in the Figure 21. Again loops are not shown.

Proposition 3.2.5. $\overline{\text{Aut}}(\rho_{23}^7)$ is generated by $\beta_0, \beta_2, \beta_4, \beta_5$, and δ_4 .

Proof. First notice that $\overline{\text{Aut}}(\rho_{23}^7) = \pi_1(\mathcal{C}(\rho_{23}^7), \rho_{23}^7)$ is generated by *lassoes*, i.e. elements of the form wxw^{-1} where, w is a path not containing loops (that is, w is a subtree) starting at ρ_{23}^7 and x is a loop at the endpoint of w . Furthermore the tail w is not important: two lassoes with the same head (at the same vertex with the same label) represent the same element.

This is clear from Figure 21 and Proposition 3.1.9.

By Proposition 3.2.3 one only needs to check lassoes with

FIGURE 21. $\mathcal{C}(\rho_{23}^7)$ (a) heads at $\tilde{\rho}_4^7$ The heads are labelled by β_0 or β_2 . Using the path $w = \beta_3\beta_4\beta_5\beta_2\beta_3\delta_4$ one gets:

$$w\beta_0w^{-1} = \beta_0$$

$$\begin{aligned} w\beta_2w^{-1} &= [\beta_2]\delta_4^{-1}\beta_3^{-1}\beta_2^1\beta_5^{-1}\beta_4^{-1}\beta_3^{-1} \\ &= [\beta_2]\beta_3^{-1}\beta_2^1\beta_5^{-1}\beta_4^{-1}\beta_3^{-1} \\ &= [\beta_3]B_5^{-1}\beta_4^{-1}\beta_3^{-1} \\ &= [\beta_3]\beta_4^{-1}\beta_3^{-1} \\ &= \beta_4 \end{aligned}$$

(b) The lasso with head at $\tilde{\rho}_3^6$ labelled by β_4 (corresponding to $[\beta_4]\beta_3^{-1}$).Using the path $w = \beta_3\beta_4\beta_5\beta_2\delta_4$ one gets:

$$\begin{aligned} w\beta_4w^{-1} &= [\beta_4]\delta_4^{-1}\beta_2^1\beta_5^{-1}\beta_4^{-1}\beta_3^{-1} \\ &= [\beta_4]\beta_5^{-1}\beta_4^{-1}\beta_3^{-1} \\ &= [\beta_5]\beta_3^{-1} \\ &= \beta_5 \end{aligned}$$

(c) heads labelled by β_5 In this case the head is either in $i_{(23)}(\mathcal{C}(\rho_{23}^6))$ or in $i_{(14)}(\mathcal{C}(\rho_2^6))$.In the first case its obvious that both of them are equal to β_5 since one can choose the path w to lie entirely inside $i_{(23)}(\mathcal{C}(\rho_{23}^6))$ and therefore all it's edges to commute with β_5 .In the second case one only needs to check those with head at ρ_5^7 and $\tilde{\rho}_2^7$.

For the first use the path $w = \beta_3\beta_2\beta_4\beta_3\beta_5\beta_4$ to get:

$$\begin{aligned} w\beta_5w^{-1} &= [\beta_5]\beta_4^{-1}\beta_5^{-1}\beta_3^{-1}\beta_4^{-1}\beta_2^{-1}\beta_3^{-1} \\ &= [\beta_4]\beta_3^{-1}\beta_4^{-1}\beta_2^{-1}\beta_3^{-1} \\ &= [\beta_3]\beta_2^{-1}\beta_3^{-1} \\ &= \beta_2. \end{aligned}$$

For the second use the path $w = \beta_3\beta_4\beta_5\delta_4$ to get:

$$\begin{aligned} w\beta_5w^{-1} &= [\beta_5]\delta_4^{-1}\beta_5^{-1}\beta_4^{-1}\beta_3^{-1} \\ &= [\delta_4]\beta_4^{-1}\beta_3^{-1} \\ &= \delta_4 \end{aligned}$$

(d) heads at $\tilde{\rho}_6^7$.

Those have heads labelled by β_2 , or β_4 , or δ_4 .

For the first one use any path to see that it is equal to a lasso with head at $\tilde{\rho}_5^7$, labelled by β_2 . The later has been checked in case a).

For the second one use a path that ends with $\beta_4\beta_5$ say $w = w'\beta_4\beta_5$ to get:

$$w'\beta_4\beta_5\beta_4\beta_5^{-1}\beta_4^{-1}(w')^{-1} = w'\beta_5(w')^{-1}$$

which has head at $\tilde{\rho}_5^7$ and therefore has been checked in b). (It turns out to be δ_4).

Finally for the third one use a path of the form $w = w'\delta_4\beta_5$ to get:

$$w'\delta_4\beta_5\delta_4\beta_5^{-1}\delta_4^{-1}(w')^{-1} = w'\beta_5(w')^{-1}$$

which has head at ρ_5^7 and therefore has been checked in b). (It turns out to be β_2).

□

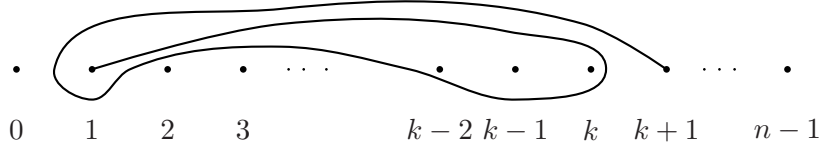
Lemma 3.2.6. *The fundamental group of \mathcal{C}_\bullet^n is generated by lassoes. Furthermore the tail of a lasso is not important: two lassoes based at the same vertex and having the same head (at the same vertex labelled by the same element) are equal.*

Proof. Attach 2-cells to kill all loops. It suffices to prove that the resulting complex $\bar{\mathcal{C}}_\bullet^n$ is simply connected. By induction on the number of branch values n : It is true for $n = 6, 7$. Assume it is true for all smaller values of n . Then by Lemmas 3.1.7 and 3.1.9 $\bar{\mathcal{C}}_{\text{id}}^n$ is the union of two simply connected complexes glued along a connected subcomplex and therefore by Van Kampen's theorem it is simply connected. The second statement follows from the fact that the intersection of the two pieces is actually simply connected.

The proof for $\mathcal{C}_{(23)}^n$ and $\mathcal{C}_{(14)(23)}^n$ is the same after observing that the extra vertices are glued along isolated edges.

□

Definition 3.2.7. For even k , d_k is the interval shown in Figure 22 and δ_k is the rotation around d_k .

FIGURE 22. The interval d_k

Lemma 3.2.8. *Let G be the subgroup of B_n generated by the elements listed in Theorem 3.2.2. Then δ_k is in G for all k .*

Proof. It is clear that δ_k is in $L(n)$. Now notice that for $k \geq 6$, δ_k fixes pointwise a small disc containing A_2 and A_3 but no other branch value. Connect this disc to ∂D^2 by an arc that misses the A_i 's, the α_i 's and the x_i 's. Remove the disc and the arc to get a *three-sheeted* covering of a disk which is equivalent to $\rho(n-2)$ via an equivalence that sends d_6 to d_4 . Apply Theorem 2.1.1 to this covering and then glue the disk and the arc back in to get an expression of δ_k as a word in the generators of G . \square

Proof of 3.2.2. The cases $n = 6$, $n = 7$ have been proved already. Let $n \geq 8$ and assume the theorem proven for all smaller values of n .

By 3.2.6 suffices to prove that all lassoes are in G where where G is the subgroup of $\overline{\text{Aut}}$ generated by the listed elements.

If n is even then (at the level of 0-skeletons)

$$\begin{aligned} \mathcal{C}(\rho_{23}^n) &= \mathcal{C}_{\text{id}}^n \\ &= i_{(23)}(\mathcal{C}_{(23)}^{n-1}) \sqcup i_{(14)}(\mathcal{C}_{(14)}^{n-1}) \end{aligned}$$

and the lassoes fall in to two cases:

Case a: Lassoes with heads at $i_{(23)}(\mathcal{C}_{(23)}^{n-1})$.

In this case by the induction hypothesis, one needs only to check lassoes with head labelled by β_{n-2} . After writing

$$\mathcal{C}_{(23)}^{n-1} = i_{(23)}(\mathcal{C}_{\text{id}}^{n-2} \sqcup \{\tilde{\rho}_\emptyset^{n-2}\}) \sqcup i_{(14)}(\mathcal{C}_{(14)(23)}^{n-2})$$

and observing that for lassoes in $i_{(23)}i_{(23)}(\mathcal{C}_{\text{id}}^{n-2})$ the tail can be chosen to commute with β_{n-2} , one is left with checking the lasso with head at $\tilde{\rho}_{n-2,n-1}^n$ labelled by β_{n-2} .

If $n = 8$ notice that the path $w = \beta_5\delta_4\beta_6\beta_5$ connects ρ_{56}^8 to $\tilde{\rho}_{56}^8$ and

$$\begin{aligned} w\beta_6w^{-1} &= \beta_5\delta_4\beta_6\beta_5\beta_6\beta_5^{-1}\beta_6^{-1}\delta_4^{-1}\beta_5^{-1} \\ &= \beta_5\delta_4\beta_5\delta_4^{-1}\beta_5^{-1} \\ &= \delta_4 \end{aligned}$$

so that the lasso with head at $\tilde{\rho}_{56}^8$ labelled by β_6 is equal to the lasso with head at ρ_{56}^8 labelled by δ_4 . The later is by definition equal to δ_6 , since the path $\beta_3\beta_4\beta_5\beta_6\beta_2\beta_3\beta_4\beta_5$ connects ρ_{23}^8 to ρ_{56}^8 .

If $n \geq 10$ notice that the path $w = \delta_{n-2}\beta_{n-4}\beta_{n-5}\beta_{n-3}\beta_{n-4}\beta_{n-2}\beta_{n-3}$ connects $\tilde{\rho}_{n-5,n-3,n-2,n-1}^n$ to $\tilde{\rho}_{n-2,n-1}$ and

$$\begin{aligned} w\beta_{n-2}w^{-1} &= [\beta_{n-2}]\beta_{n-3}^{-1}\beta_{n-2}^{-1}\beta_{n-4}^{-1}\beta_{n-3}^{-1}\beta_{n-5}^{-1}\beta_{n-4}^{-1}\delta_{n-2}^{-1} \\ &= [\beta_{n-3}]\beta_{n-4}^{-1}\beta_{n-3}^{-1}\beta_{n-5}^{-1}\beta_{n-4}^{-1}\delta_{n-2}^{-1} \\ &= [\beta_{n-4}]\beta_{n-5}^{-1}\beta_{n-4}^{-1}\delta_{n-2}^{-1} \\ &= [\beta_{n-5}]\delta_{n-2}^{-1} \end{aligned}$$

and therefore by the induction hypothesis (since $\tilde{\rho}_{n-5,n-3,n-2,n-1}^n \in i_{(23)}(\mathbb{C}_{(23)}^{n-1})$) the lasso with head at $\tilde{\rho}_{n-2,n-1}$ labelled by β_{n-2} is indeed in G .

Case b: Lassoes with heads at $i_{(14)}(\mathbb{C}_{(14)}^{n-1})$.

By symmetry and the previous case one needs to check only lassoes with head at $\tilde{\rho}_{23}^n$ and when $n \geq 10$ the lasso with head at $\tilde{\rho}_{56}^n$ labelled by β_{n-2} (corresponding to δ_6).

For the lassoes based at $\tilde{\rho}_{23}^n$ and head labelled by $\beta_2, \beta_4, \beta_5, \dots, \beta_{n-2}$ notice that the path $w = \beta_{n-3}\beta_{n-4} \cdots \beta_2\beta_{n-2}\beta_{n-3} \cdots \beta_3$ connects $\tilde{\rho}_{n-2,n-1}^n$ to $\tilde{\rho}_{23}^n$ and

$$\begin{aligned} w\beta_2w^{-1} &= [\beta_2]\beta_3^{-1}\beta_4^{-1} \cdots \beta_{n-3}^{-1}\beta_{n-2}^{-1}\beta_2^{-1}\beta_2^{-1}\beta_3^{-1} \cdots \beta_{n-4}^{-1}\beta_{n-3}^{-1} \\ &= [\beta_2]\beta_3^{-1}\beta_2^{-1}\beta_4^{-1} \cdots \beta_{n-3}^{-1}\beta_{n-2}^{-1}\beta_2^{-1}\beta_3^{-1} \cdots \beta_{n-4}^{-1}\beta_{n-3}^{-1} \\ &= [\beta_3]\beta_4^{-1} \cdots \beta_{n-3}^{-1}\beta_{n-2}^{-1}\beta_2^{-1}\beta_3^{-1} \cdots \beta_{n-4}^{-1}\beta_{n-3}^{-1} \\ &= \cdots \\ &= [\beta_{n-3}]\beta_{n-2}^{-1}\beta_{n-3}^{-1} \\ &= \beta_{n-2}. \end{aligned}$$

and (via similar calculations), for $i = 4, \dots, n-2$

$$w\beta_iw^{-1} = \beta_{i-2}.$$

Therefore by the previous case all of these lassoes belong to G .

For the lasso with head at $\tilde{\rho}_{23}^n$ labelled by δ_4 notice that the path $w = \beta_{n-2}\beta_{n-3} \cdots \beta_7\delta_4\beta_5\beta_4\beta_3$ connects $\tilde{\rho}_{3,4,5,n-1}^n$ to $\tilde{\rho}_{23}^n$ and

$$\begin{aligned} w\delta_4w^{-1} &= [\delta_4]\beta_3^{-1}\beta_4^{-1}\beta_5^{-1}\delta_4^{-1}\beta_7^{-1} \cdots \beta_{n-3}^{-1}\beta_{n-2}^{-1} \\ &= [\delta_4]\beta_5^{-1}\delta_4^{-1} \\ &= \beta_5 \end{aligned}$$

and therefore since $\tilde{\rho}_{3,4,5,n-1}^n \in i_{(23)}(\mathbb{C}_{(23)}^{n-1})$ by case a) this lasso is in G .

For the lasso with head at $\tilde{\rho}_{56}^n$ labelled by β_{n-2} notice that the path $w = \beta_{n-2}\beta_{n-3} \cdots \beta_7$ connects $\tilde{\rho}_{5,n-1}^n$ to $\tilde{\rho}_{56}^n$ and

$$\begin{aligned} w\beta_{n-2}w^{-1} &= [\beta_{n-2}]\beta_7^{-1} \cdots \beta_{n-3}^{-1}\beta_{n-2}^{-1} \\ &= [\beta_{n-2}]\beta_{n-3}^{-1}\beta_{n-2}^{-1} \\ &= \beta_{n-3}. \end{aligned}$$

and therefore since $\tilde{\rho}_{5,n-1}^n \in i_{(23)}(\mathcal{C}_{(23)}^{n-1})$ by case a) this lasso is in G . This concludes the proof for $\overline{\text{Aut}}(\rho_{23}^n)$ when n is even.

Continuing with n even:

$$\begin{aligned} \mathcal{C}(\rho_{2,3,n-1}^n) &= \mathcal{C}_{(23)}^n \\ &= i_{(23)}(\mathcal{C}_{(14)}^{n-1} \sqcup \{\rho_{\emptyset}^{n-1}\}) \bigsqcup i_{(14)}(\mathcal{C}_{(23)}^{n-1} \sqcup \{\tilde{\rho}_{\emptyset}^{n-1}\}) \end{aligned}$$

and the lassoes fall in to four cases:

Case a: Lassoes with heads at $i_{(14)}(\mathcal{C}_{(23)}^{n-1})$.

In this case by the induction hypothesis one only needs to check lassoes with head labelled by β_{n-2} . But those actually have heads lying inside $i_{(14)}i_{(14)}(\mathcal{C}_{(14)(23)}^{n-2})$ which is connected and all of its edges commute with β_{n-2} . It therefore follows that all of these lassoes are equal to the lasso with head at $\rho_{2,n-2,n-1}^n$ labelled by β_{n-2} . Noticing that the path $w = \beta_3\beta_4 \cdots \beta_{n-3}$ connects $\rho_{2,3,n-1}^n$ to $\rho_{2,n-2,n-1}^n$ one sees that the later lasso equals $[\beta_{n-2}]\beta_{n-3}^{-1} \cdots \beta_3^{-1}$.

Case b: Lassoes with heads at ρ_{n-1}^n .

Using as tail the path $w = \beta_{n-2}\beta_{n-3} \cdots \beta_5\delta_4\beta_4\beta_5 \cdots \beta_{n-2}$ one sees that:

$$\begin{aligned} w\beta_0w^{-1} &= [\beta_0]\beta_{n-2}^{-1}\beta_{n-3}^{-1} \cdots \beta_5^{-1}\beta_4^{-1}\delta_4^{-1}\beta_5^{-1} \cdots \beta_{n-3}^{-1}\beta_{n-2}^{-1} \\ &= \beta_0 \end{aligned}$$

$$\begin{aligned} w\beta_2w^{-1} &= [\beta_2]\beta_{n-2}^{-1}\beta_{n-3}^{-1} \cdots \beta_5^{-1}\beta_4^{-1}\delta_4^{-1}\beta_5^{-1} \cdots \beta_{n-3}^{-1}\beta_{n-2}^{-1} \\ &= \beta_2 \end{aligned}$$

$$\begin{aligned} w\beta_3w^{-1} &= [\beta_3]\beta_{n-2}^{-1}\beta_{n-3}^{-1} \cdots \beta_5^{-1}\beta_4^{-1}\delta_4^{-1}\beta_5^{-1} \cdots \beta_{n-3}^{-1}\beta_{n-2}^{-1} \\ &= [\beta_3]\beta_4^{-1}\delta_4^{-1}\beta_5^{-1} \cdots \beta_{n-3}^{-1}\beta_{n-2}^{-1} \\ &= [\beta_3]\delta_4^{-1}\beta_4^{-1}\beta_5^{-1} \cdots \beta_{n-3}^{-1}\beta_{n-2}^{-1} \\ &= [\beta_3]\beta_4^{-1}\beta_5^{-1} \cdots \beta_{n-3}^{-1}\beta_{n-2}^{-1} \end{aligned}$$

which as seen in Figure 23 equals $[\beta_{n-2}]\beta_{n-3}^{-1}\beta_{n-4}^{-1} \cdots \beta_4^{-1}$.

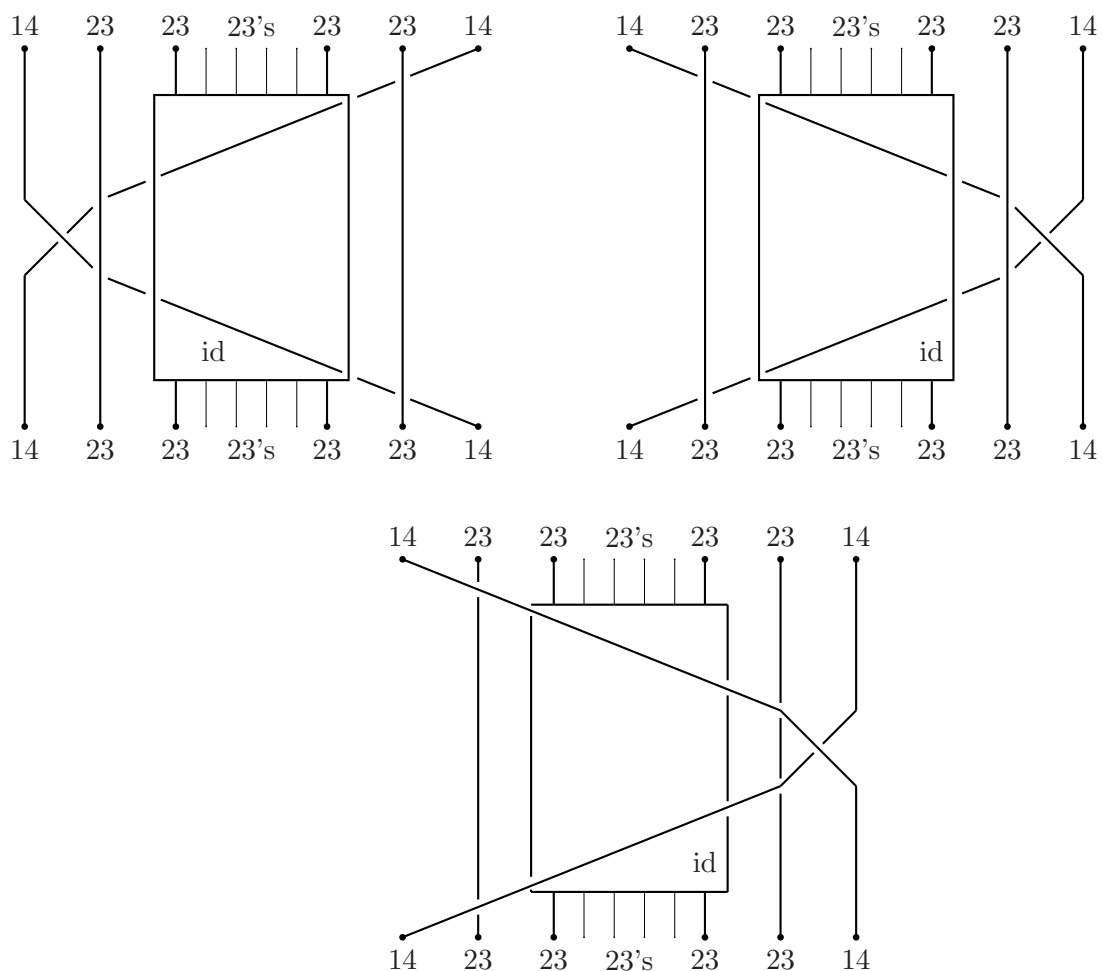


FIGURE 23. First shift to the right place by isotopy and then use move \mathcal{P} to pass over the strands in the box.

$$\begin{aligned}
 w\beta_4w^{-1} &= [\beta_4]\beta_{n-2}^{-1}\beta_{n-3}^{-1}\cdots\beta_5^{-1}\beta_4^{-1}\delta_4^{-1}\beta_5^{-1}\cdots\beta_{n-3}^{-1}\beta_{n-2}^{-1} \\
 &= [\beta_4]\beta_5^{-1}\beta_4^{-1}\delta_4^{-1}\beta_5^{-1}\cdots\beta_{n-3}^{-1}\beta_{n-2}^{-1} \\
 &= [\beta_5]\delta_4^{-1}\beta_5^{-1}\cdots\beta_{n-3}^{-1}\beta_{n-2}^{-1} \\
 &= [\delta_4]\beta_6^{-1}\cdots\beta_{n-3}^{-1}\beta_{n-2}^{-1} \\
 &= \delta_4
 \end{aligned}$$

$$\begin{aligned}
w\delta_4w^{-1} &= [\delta_4]\beta_{n-2}^{-1}\beta_{n-3}^{-1}\cdots\beta_5^{-1}\beta_4^{-1}\delta_4^{-1}\beta_5^{-1}\cdots\beta_{n-3}^{-1}\beta_{n-2}^{-1} \\
&= [\delta_4]\beta_5^{-1}\beta_4^{-1}\delta_4^{-1}\beta_5^{-1}\cdots\beta_{n-3}^{-1}\beta_{n-2}^{-1} \\
&= [\delta_4]\beta_5^{-1}\delta_4^{-1}\beta_4^{-1}\beta_5^{-1}\cdots\beta_{n-3}^{-1}\beta_{n-2}^{-1} \\
&= [\beta_5]\beta_4^{-1}\beta_5^{-1}\cdots\beta_{n-3}^{-1}\beta_{n-2}^{-1} \\
&= [\beta_4]\beta_6^{-1}\cdots\beta_{n-3}^{-1}\beta_{n-2}^{-1} \\
&= \beta_4
\end{aligned}$$

$$\begin{aligned}
w\beta_5w^{-1} &= [\beta_5]\beta_{n-2}^{-1}\beta_{n-3}^{-1}\cdots\beta_5^{-1}\beta_4^{-1}\delta_4^{-1}\beta_5^{-1}\cdots\beta_{n-3}^{-1}\beta_{n-2}^{-1} \\
&= [\beta_5]\beta_6^{-1}\beta_5^{-1}\beta_4^{-1}\delta_4^{-1}\beta_5^{-1}\cdots\beta_{n-3}^{-1}\beta_{n-2}^{-1} \\
&= [\beta_6]\delta_4^{-1}\beta_4^{-1}\beta_5^{-1}\cdots\beta_{n-3}^{-1}\beta_{n-2}^{-1} \\
&= [\beta_6]\beta_5^{-1}\beta_6^{-1}\cdots\beta_{n-3}^{-1}\beta_{n-2}^{-1} \\
&= [\beta_5]\beta_7^{-1}\cdots\beta_{n-3}^{-1}\beta_{n-2}^{-1} \\
&= \beta_5
\end{aligned}$$

and similarly for $i = 6, \dots, \beta_{n-3}$

$$w\beta_iw^{-1} = \beta_i$$

Case c: Lassoes with heads at $i_{(23)}(\mathbb{C}_{(14)}^{n-1})$.

By symmetry and case a) one needs only to check lassoes with head at $\tilde{\rho}_{2,3,n-1}^n$, the lasso with head at $\tilde{\rho}_{2,n-2,n-1}$ labelled by β_{n-2} (corresponding to $[\beta_{n-2}]\beta_{n-3}^{-1}\cdots\beta_3^{-1}$), and for $n \geq 10$ the lasso with head at $\tilde{\rho}_{2,3,n-1}^n$ labelled by δ_4 (corresponding to δ_6).

For the lassoes with head at $\tilde{\rho}_{2,3,n-1}^n$ labelled by δ_4 or β_i for $i = 2, 4, 5, \dots, \beta_{n-4}$ notice that β_{n-2} connects $\tilde{\rho}_{2,3,n-1}^n$ to $\tilde{\rho}_{2,3,n-2}^n \in i_{(14)}(\mathbb{C}_{(12)}^{n-1})$ and so they have been checked in case a).

For the one with head labelled by β_{n-3} “pull further into $i_{(14)}(\mathbb{C}_{(12)}^{n-1})$ ” by using the path $\beta_{n-2}\beta_{n-3}$.

For the lasso with head at $\tilde{\rho}_{2,n-2,n-1}$ labelled by β_{n-2} use again the path $\beta_{n-2}\beta_{n-3}$ to “pull it” to the lasso with head at $\tilde{\rho}_{2,n-3,n-2} \in i_{(14)}(\mathbb{C}_{(12)}^{n-1})$, labelled by β_{n-3} .

Finally for the lasso with head at $\tilde{\rho}_{2,3,n-1}^n$ labelled by δ_4 use β_{n-2} to “pull” it to $\tilde{\rho}_{2,3,n-1}^n \in i_{(14)}(\mathbb{C}_{(23)}^{n-1})$ with label δ_4 .

Case d: Lassoes with heads at $\tilde{\rho}_{n-1}^n$.

Analogously to case b) those are covered by case c).

This concludes the proof for $\overline{\text{Aut}}(\rho_{2,3,n-1}^n)$ and the even n case.

For odd n :

$$\begin{aligned}
\mathcal{C}(\rho_{23}^n) &= \mathcal{C}_{(23)}^n \\
&= i_{(23)}(\mathbb{C}_{\text{id}}^{n-1} \sqcup \{\tilde{\rho}_\emptyset^{n-1}\}) \bigsqcup i_{(14)}(\mathbb{C}_{(14)(23)}^{n-1})
\end{aligned}$$

and the lassoes fall into three cases:

Case a: Lassoes with heads at $i_{(23)}(\mathbb{C}_{\text{id}}^{n-1})$

In this case by the induction hypothesis, one needs only to check lassoes with head labelled by β_{n-2} . After writing

$$\mathbb{C}_{\text{id}}^{n-1} = i_{(23)}(\mathbb{C}_{(23)}^{n-2}) \bigsqcup i_{(14)}(\mathbb{C}_{(14)}^{n-2})$$

and observing that for lassoes in $i_{(23)}i_{(23)}(\mathbb{C}_{(23)}^{n-2})$ the tail can be chosen to commute with β_{n-2} , one sees that all of these lassoes are equal to β_{n-2} .

Case b: Lassoes with heads at $i_{(14)}(\mathbb{C}_{(14)(23)}^{n-1})$

By the induction hypothesis one needs only to check the lassoes with heads at $\rho_{2,3,n-2,n-1}$, the lasso with head at $\rho_{2,n-3,n-2,n-1}$ labelled by β_{n-3} , and the lasso with head at $\rho_{5,6,n-2,n-1}$ labelled by δ_4 .

For the lassoes with head at $\rho_{2,3,n-2,n-1}$ labelled by δ_4 or by β_i with $i = 2, 4, 5, \dots, \beta_{n-5}$ use the path $\beta_{n-2}\beta_{n-3}$ to pull them at $\rho_{2,3,n-3,n-2} \in i_{(23)}(\mathbb{C}_{\text{id}}^{n-1})$ with the same label and refer to case a).

For the lasso with head at $\rho_{2,3,n-2,n-1}$ labelled by β_{n-2} use the path $\beta_{n-2}\beta_{n-3}$ to pull it at $\rho_{2,3,n-3,n-2} \in i_{(23)}(\mathbb{C}_{\text{id}}^{n-1})$ with label β_{n-3} and refer to case a).

For the lasso with head at $\rho_{2,3,n-2,n-1}$ labelled by β_{n-4} use the path $\beta_{n-3}\beta_{n-2}\beta_{n-4}\beta_{n-3}$ to pull it at $\rho_{2,3,n-4,n-3} \in i_{(23)}(\mathbb{C}_{\text{id}}^{n-1})$ with label β_{n-2} and refer to case a).

For the lasso with head at $\rho_{2,n-3,n-2,n-1}$ labelled by β_{n-3} , use the path $\beta_{n-2}\beta_{n-3}\beta_{n-4}$ to pull it at $\rho_{2,n-4,n-3,n-2} \in i_{(23)}(\mathbb{C}_{\text{id}}^{n-1})$ with label β_{n-4} and refer to case a).

Finally for the lasso with head at $\rho_{5,6,n-2,n-1}$ labelled by δ_4 , use the path $\beta_{n-2}\beta_{n-3}$ to pull it at $\rho_{5,6,n-3,n-2} \in i_{(23)}(\mathbb{C}_{\text{id}}^{n-1})$ with label δ_4 and refer to case a).

Case c: Lassoes with heads at $\tilde{\rho}_{n-1}^n$

For those with heads labelled by δ_4 or β_i with $i = 1, 2, \dots, n-4$ use β_{n-2} to pull them at $\tilde{\rho}_{n-2}^n \in i_{(14)}(\mathbb{C}_{(14)(23)}^{n-1})$ with the same label, and refer to case b).

For the one with head labelled by β_{n-3} use $\beta_{n-3}\beta_{n-2}$ to pull it at $\tilde{\rho}_{n-3}^n \in i_{(14)}(\mathbb{C}_{(14)(23)}^{n-1})$ with label β_{n-2} , and refer to case b). □

3.3. The Kernel. In this subsection we compute the kernel of the the (quotiented) lifting homomorphism in a way completely analogous to [4], see Section 2.1.

For this subsection covering means a covering over S^2 , in particular the number of branch values of a covering is even. Also notation is simplified by writing ρ_n instead of ρ_{23}^n . Then using the Riemann-Hurwitz formula one gets that the total space of ρ_n has genus

$$g = \frac{n-6}{2}.$$

In fact Figure 24 shows an explicit model of ρ_{2g+6} as a genus- g surface. This model is constructed by cutting and pasting. S^2 is cut open along the intervals x_i for even i . The cuts are shown in blue and it is assumed that the boundary circles in this picture are “sewed” to become intervals.

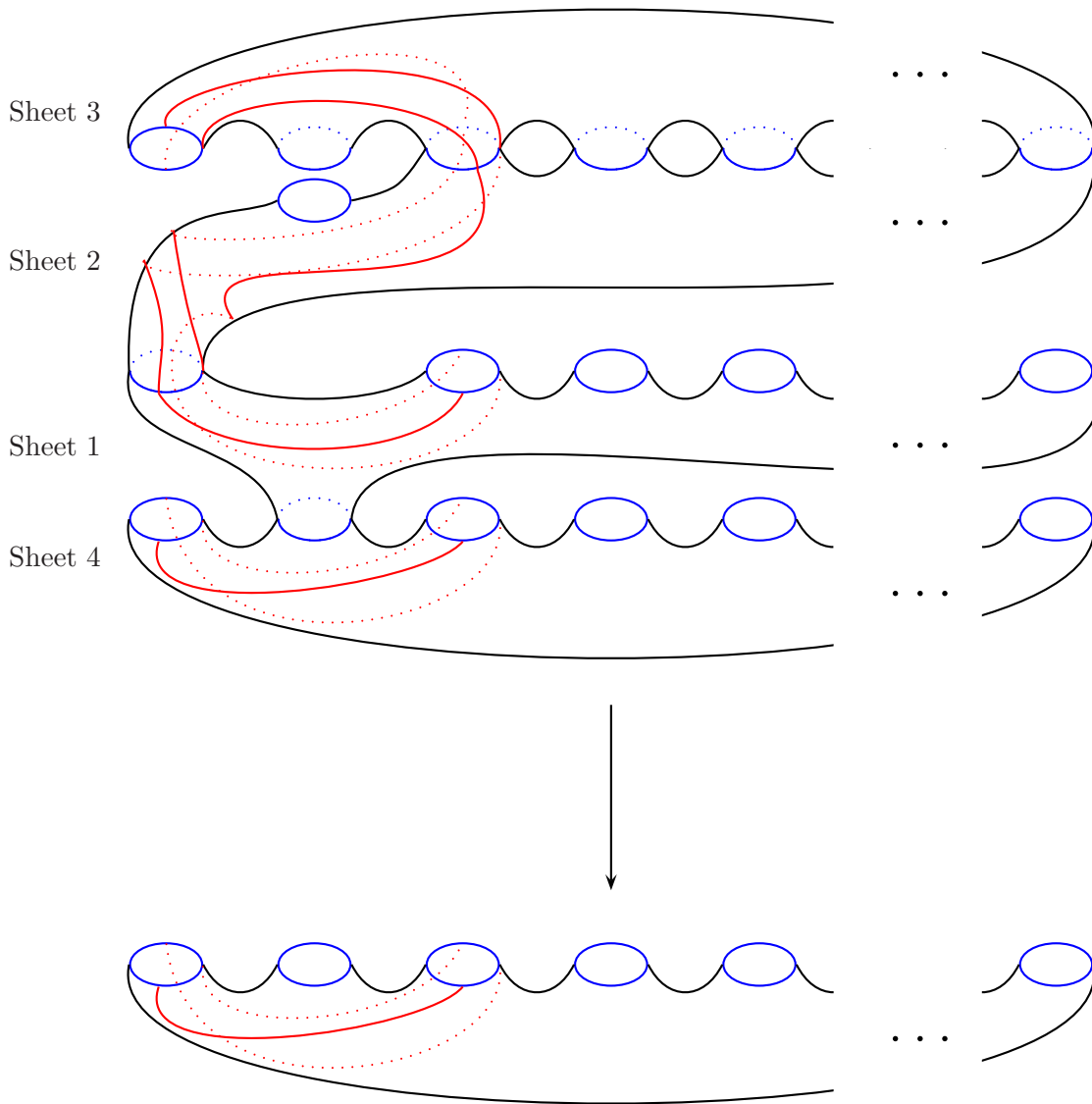


FIGURE 24. The covering ρ_n and how d_4 lifts

The commutative diagram (1.2.3) then becomes:

$$\begin{array}{ccc}
\text{Aut}(\rho_{2g+6}) & \xrightarrow{\lambda} & \mathfrak{M}_g \\
\downarrow & \nearrow \bar{\lambda} & \\
\overline{\text{Aut}}(\rho_{2g+6}) & &
\end{array}$$

Notice that all the generators of $\overline{\text{Aut}}(\rho_n)$ given in Theorem 3.2.1 are rotations around intervals and thus their image under $\bar{\lambda}$ can be determined according to Lemma 1.2.2 by lifting the intervals. Using the model for ρ_{2g+6} in Figure 24 one gets the following:

Theorem 3.3.1. $\bar{\lambda}$ is determined by:

$$(3.3.1) \quad \bar{\lambda}(x) = \begin{cases} id & \text{if } x = \beta_0, \beta_2 \\ a_{i-1} & \text{if } x = \beta_{2i} \text{ for } i \geq 2 \\ b_{i-1} & \text{if } x = \beta_{2i+1} \text{ with } i \geq 2 \\ a_1 & \text{if } x = \delta_4 \\ d & \text{if } x = \delta_6 \end{cases}$$

where a_i , b_i , and d are Wajnryb's generators of \mathfrak{M}_g as described in Appendix A.

Proof. Notice that ρ_n is obtained by $\rho(n)$ by adding a fourth trivial sheet. After ‘‘cutting off’’ the fourth sheet as in the proof of Lemma 3.2.8 d_6 becomes d_4 which as shown in Theorem 2.1.2 in the 3-sheeted case lifts to d .

In Figure 24, the interval d_4 is shown and how it lifts to the disjoint union of a curve isotopic to a_1 and two arcs.

The checks for the remaining generators are rather trivial. \square

One can now prove:

Theorem 3.3.2. *The kernel of $\bar{\lambda}$ is the smallest normal subgroup of $\overline{\text{Aut}}(\rho_{2g+6})$ containing the elements β_0 , β_2 , B , D , and all words obtained by B or D by replacing some appearances of β_4 with δ_4 , where:*

$$\begin{aligned}
B &= (\beta_4\beta_5\beta_6)^4([\delta_6^{-1}]\beta_6^{-1}\beta_5^{-1}\beta_4^{-2}\beta_5^{-1}\beta_6^{-1}\beta_7^{-1})\delta_6^{-1}, \\
D &= \beta_{2g+4}\chi\beta_{2g+4}^{-1}\chi^{-1},
\end{aligned}$$

Where:

$$\chi = \beta_{2g+3}\beta_{2g+2} \cdots \beta_5\beta_4^2\beta_5 \cdots \beta_{2g+2}\beta_{2g+3},$$

Proof. Given the Wajnryb's presentation of \mathfrak{M}_g and the fact that $\bar{\lambda}$ is given by (3.3.1) the proof reduces to checking that the words obtained by the relators in [16] after replacing in all possible ways the generators of \mathfrak{M}_g with their preimages to generators of $\overline{\text{Aut}}(\rho_{2g+6})$, are in the normal closure of the given elements.

The calculations are identical to those in Theorems 5.1 and 6.1 of [4] after replacing of x_i in [4] with β_{i+2} for $i \geq 2$, and δ_4 in [4] with δ_6 , and then replacing β_4 with δ_4 in all possible ways. \square

4. FOUR SHEETS II: COVERINGS OVER S^3

4.1. **Bi-tricolored links.** Recall from Section 1.3 how colored links represent 3-manifolds. Also recall that 4-colored links are called bi-tricolored. That name is justified by the following combinatorial description which is analogous to (but of course more complicated than) the combinatorial description of tricolored links given in Section 2.2.

Definition 4.1.1. A bi-tricolored link diagram is a link diagram whose arcs are colored by three colors that come in light and dark shades (see Section 1.4), in such a manner that:

- By disregarding the shades (i.e. dimming the lights) we get a tricolored diagram.
- There is at least one dark shade.
- At trichromatic crossings there is an even number of dark shades, while at monochromatic crossings the two pieces of the under strand have the same shade.

Recall also that a normalized (bitricolored) diagram is a link diagram in plat form whose top and bottom are equal to:

$$\rho_{\text{stand}} = \overset{12}{\frown} \quad \overset{14}{\frown} \quad \overset{23}{\frown} \quad \dots \quad \overset{23}{\frown}$$

Quite often in the next subsection a slightly different normalization will be used, namely the positions of (12)'s and (14)'s will be interchanged. The proof of Lemma 1.3.9 shows how this can be done.

4.2. **Moves.** The goal of this subsection is to prove the following two theorems:

Theorem 4.2.1. *Two bi-tricolored links represent the same 3-manifold iff they can be related by a finite sequence of moves \mathcal{M} , \mathcal{P} and the non-local moves \mathcal{X} , \mathcal{II} and \mathcal{V} shown in Figures 25, 28 and 31 respectively.*

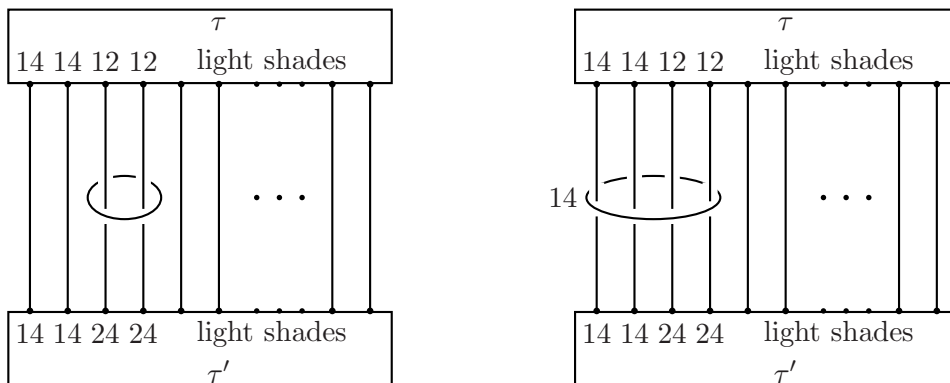


FIGURE 25. Move \mathcal{X}

Theorem 4.2.2. *Moves \mathcal{M} , \mathcal{P} plus allowing the addition/deletion of a trivial fifth sheet are enough to relate any two bi-tricolored links representing the same 3-manifold.*

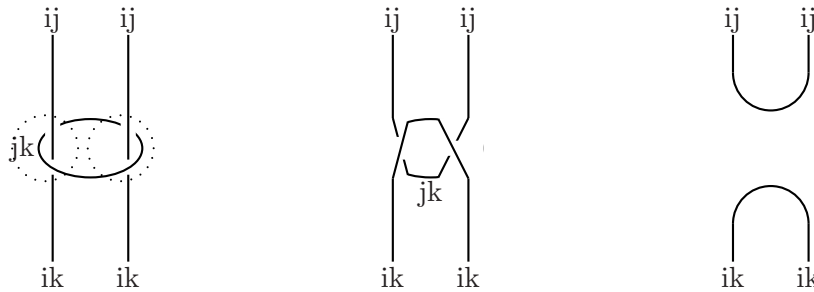
The following lemma will be used through out the proofs.

Lemma 4.2.3. *The move in Figure 26 is a consequence of move \mathcal{M} .*



FIGURE 26. The circumcision move

Proof.



Perform \mathcal{M} moves inside the dotted circles and then isotope. □

The proof proceeds in the manner of [11] and [12]. In particular we first prove the following lemma which is analogous to the main theorem of [11], see Theorem 2.2.2.

Lemma 4.2.4. *Two bi-tricolored links represent the same 3-manifold iff they can be related by a finite sequence of moves \mathcal{M} , \mathcal{P} and the non-local moves I-V shown in figures 27 through 31, where τ , τ' are arbitrary tangles with the shown endpoints.*

Proof. That moves I, II and V do not change $M(L)$ follows from the fact that the braid in their right side is in the kernel of $\bar{\lambda}$. That the moves III and IV do not change $M(L)$ follows from the fact that they can be realized by \mathcal{M} , \mathcal{P} and \mathcal{X} as shown in the proof of the theorem 4.2.1. (There is no vicious circle as this part of the argument is not used in that proof).

The proof of the reverse direction is completely analogous to Piergallini's proof of Theorem 2.2.2. Referring to the sketch of that proof given in Section 2.2 we just comment on how each step of that proof goes through in the present situation:

- Each bi-tricolored link has a normalized diagram.

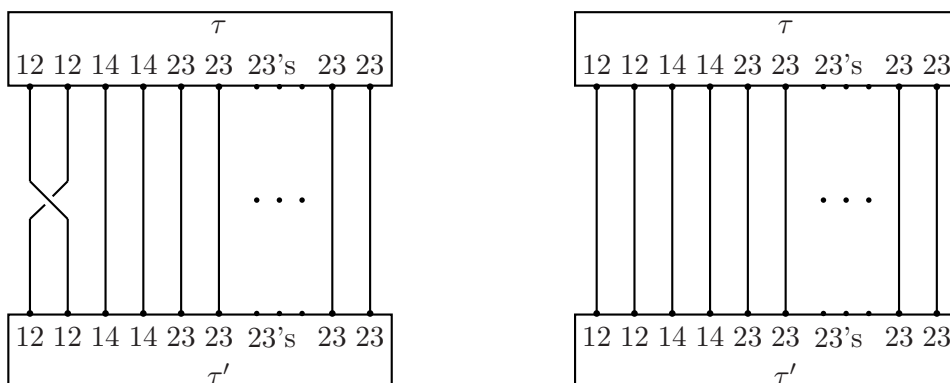


FIGURE 27. Move I

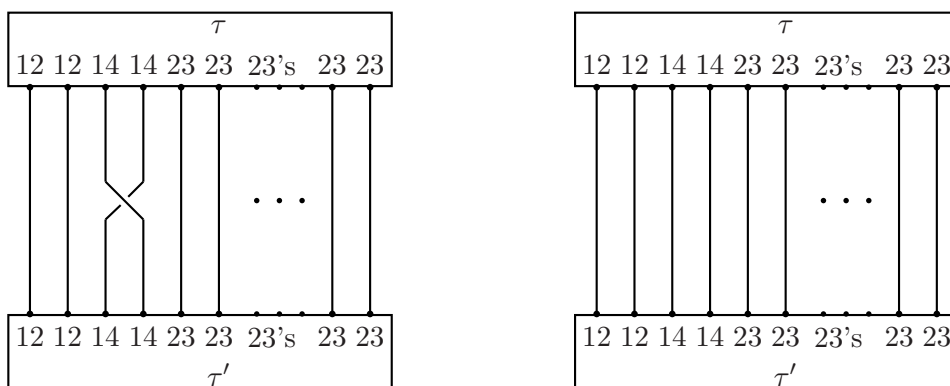


FIGURE 28. Move II

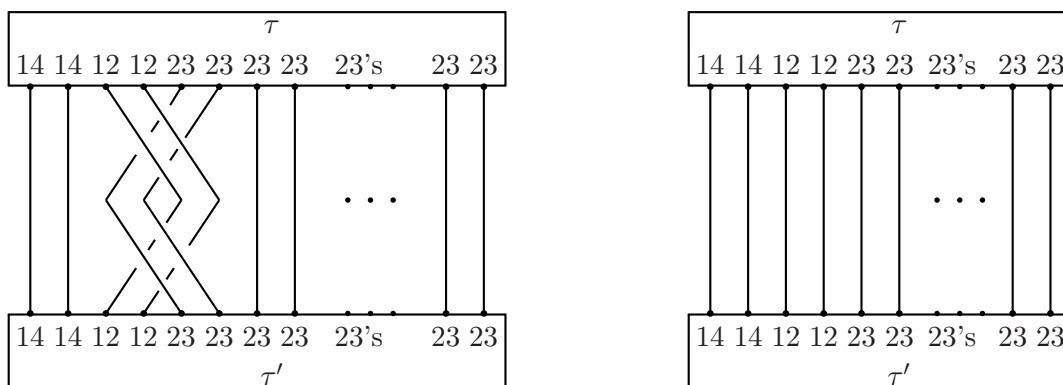


FIGURE 29. Move III

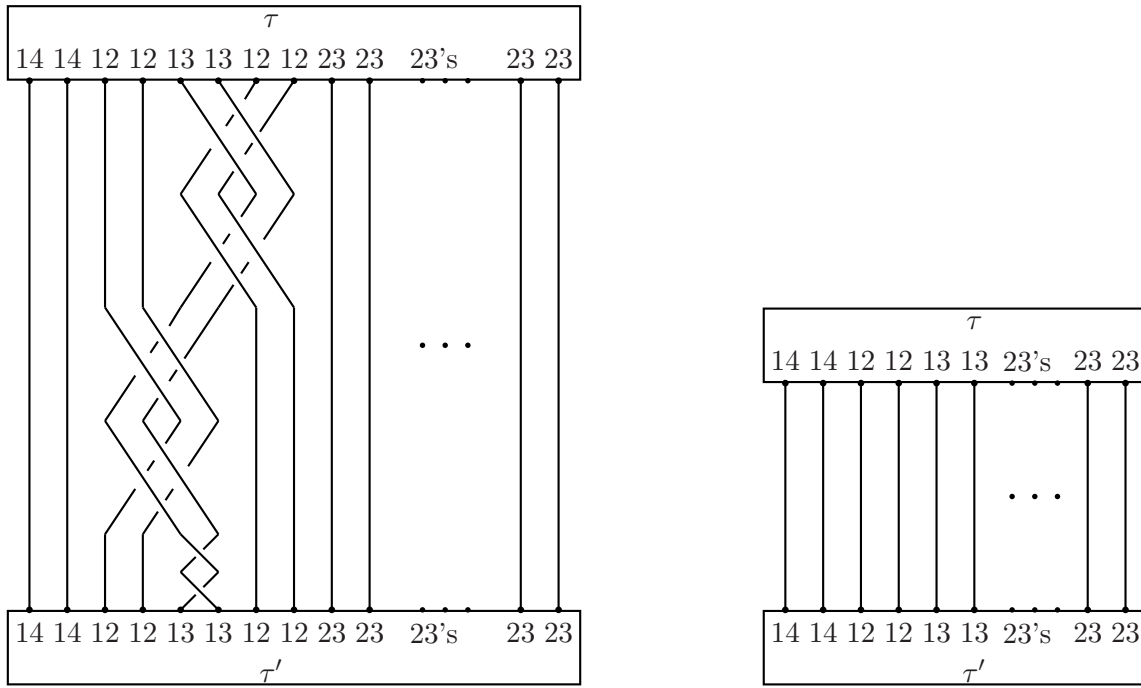


FIGURE 30. Move IV

- Step 1 (Heegard stabilization) can be realized in exactly the same way.
- For step 2, in order to get braids that lift to the Suzuki generators one just has to add two trivial strands colored by (14) to the braids Piergallini uses.
- For step 3, we have to show how to add the normal generators of $Ker \bar{\lambda}$ given in Theorem 3.3.2 to the top (and bottom) of normalized diagrams using the moves. β_0 and β_2 can be obviously added using moves I and II respectively. Also by slight modification of Piergallini's proof (by just adding two trivial strands colored by (14)) B_1 and D_1 can be added using moves \mathcal{M} , I-IV. Now move V transforms δ_4 to β_4 and therefore using move V we can transform the remaining normal generators of $Ker \bar{\lambda}$ to B or D (it easily checked that the colors are right). Thus any element of $Ker \bar{\lambda}$ can be added on the top and the bottom of a normalized diagram using the given moves.

□

Proof of 4.2.1. Moves II and V do not change $M(L)$ since the braids on their left side belong in the kernel of the lifting homomorphism $\bar{\lambda}$. That the move \mathcal{X} does not change $M(L)$ follows from the fact that it can be implemented using moves \mathcal{M} , \mathcal{P} and addition of a trivial fifth sheet as shown in the proof of theorem 4.2.2. (Again there is no vicious circle.) To show the reverse it suffices to show that the moves I through V of the previous theorem can be realized using those moves. This is done in the next few pages.

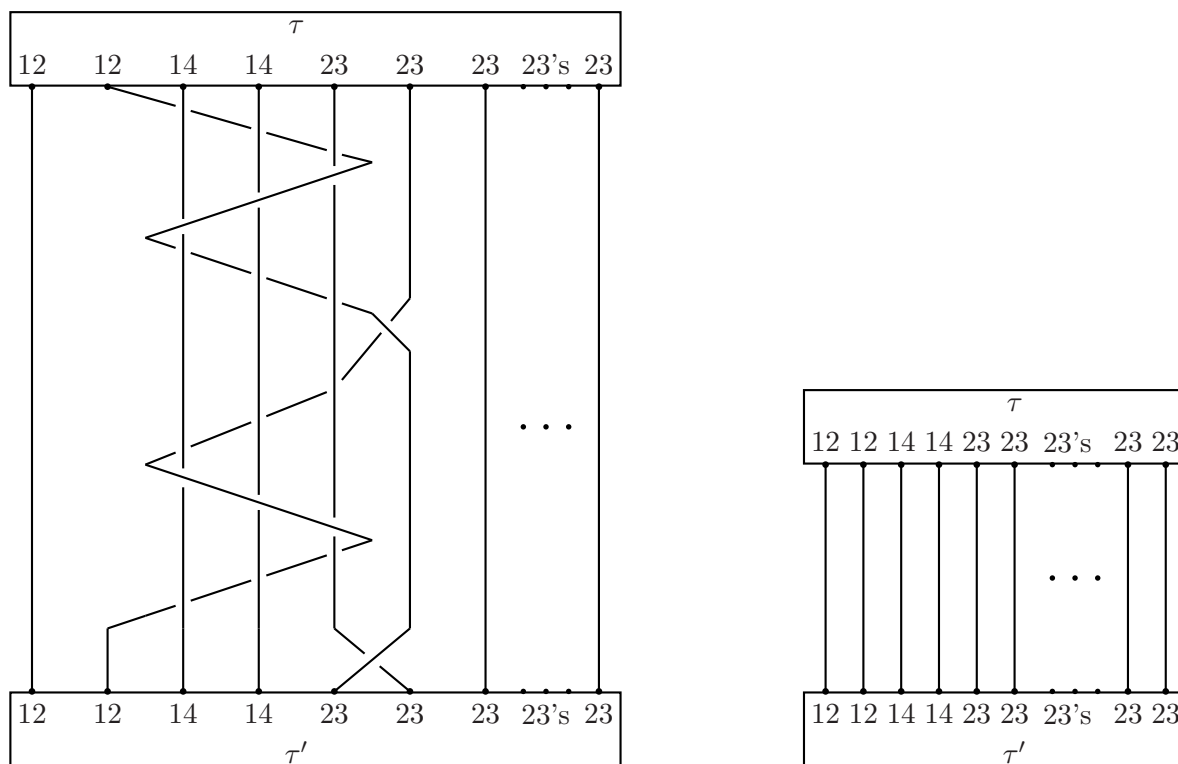
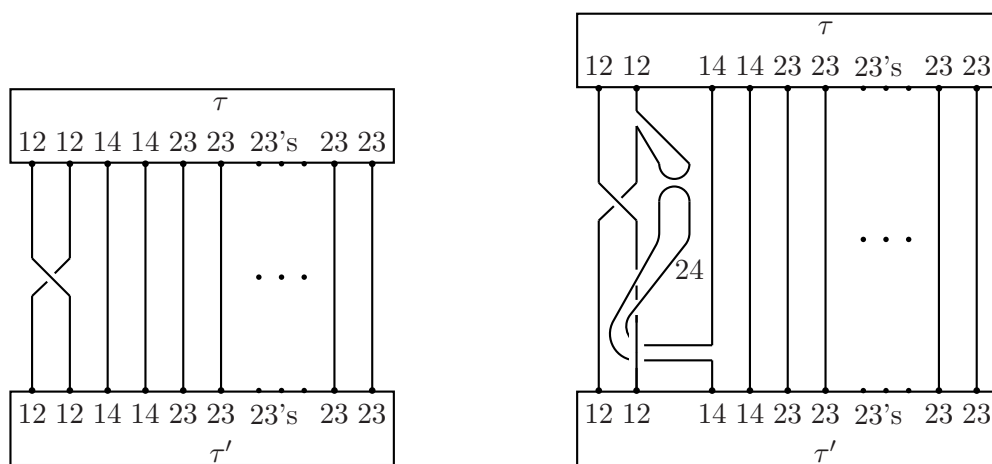
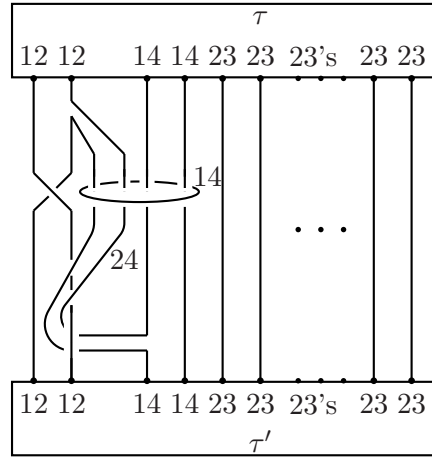
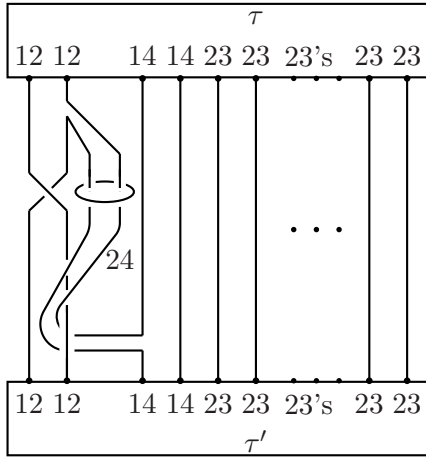


FIGURE 31. Move V

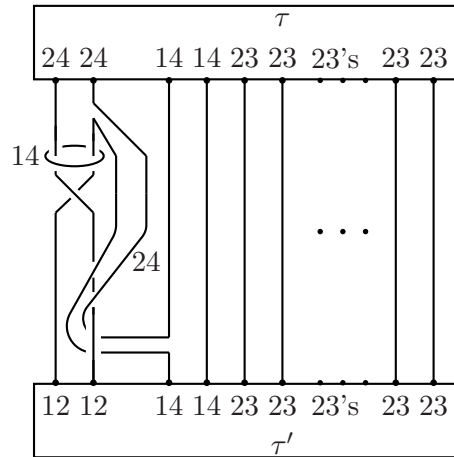
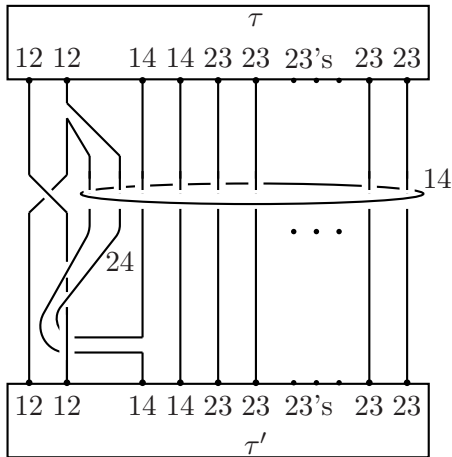
For move I:



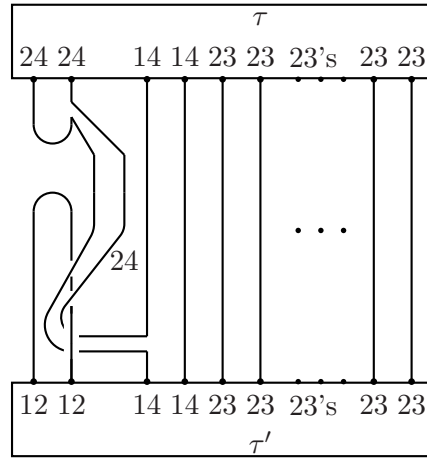
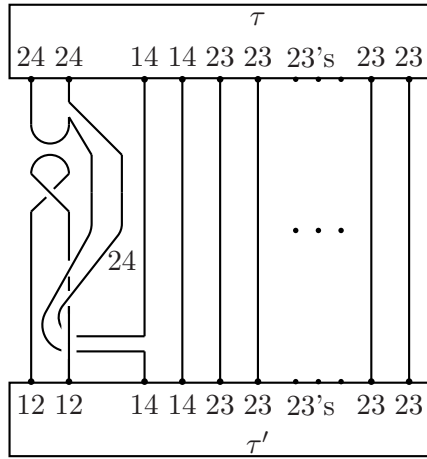
by isotopy. Then by reverse circumcision one gets:



by using move \mathcal{X} . Then by repeatedly using move \mathcal{P} one gets:

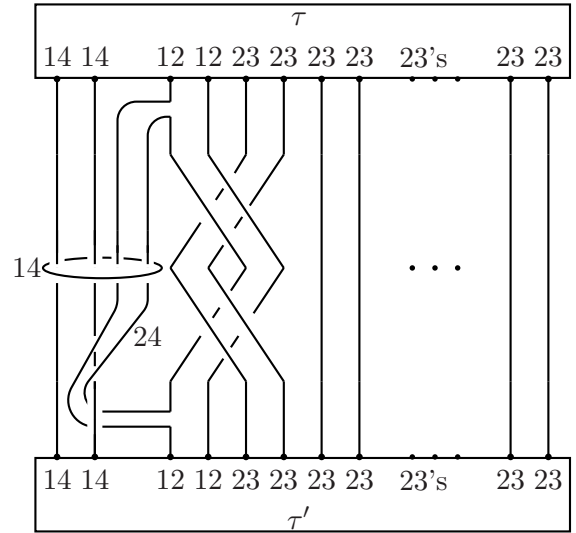
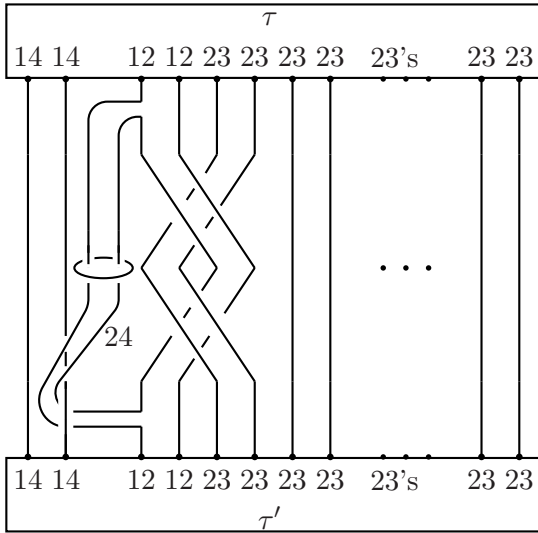


by isotopically flipping the (14)-circle over the whole diagram. Now circumcise to get:

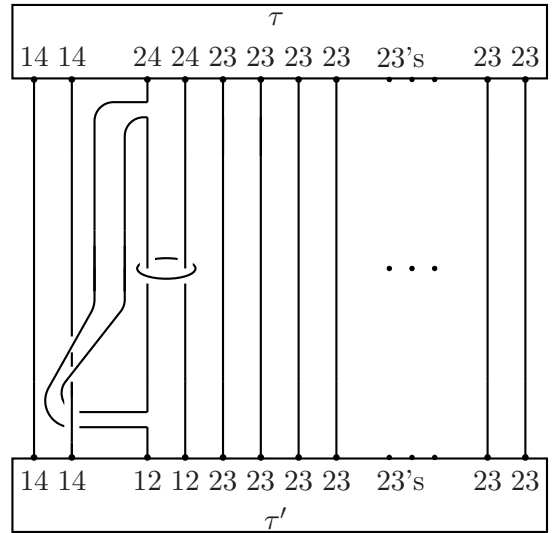
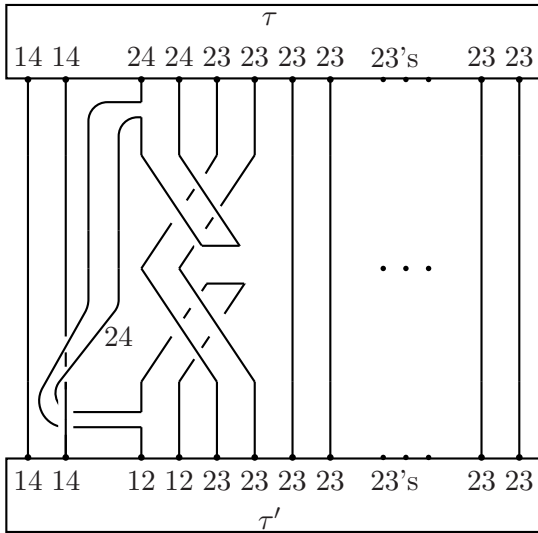


by isotopy. Now that there is no crossing reverse the process starting from the previous picture to complete move I.

For move III: Use isotopy and reverse circumcision to get:

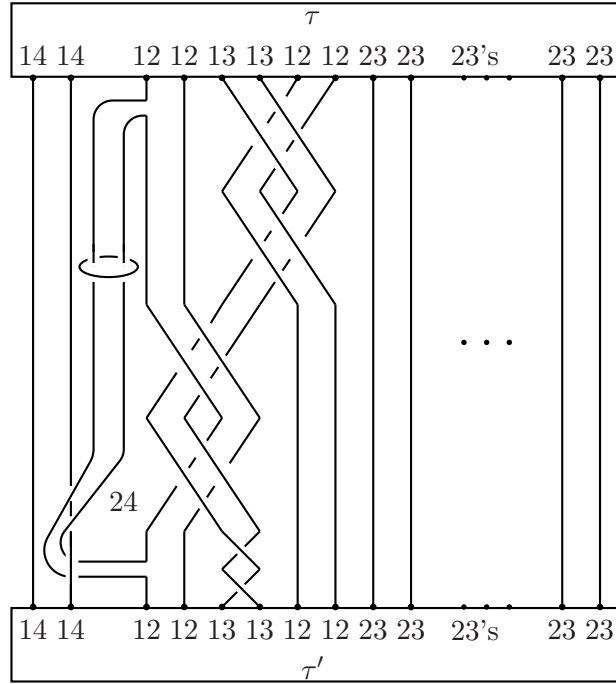


by using move \mathcal{X} . Now isotopically flip the (14)-circle over the whole diagram and apply \mathcal{P} moves to get it around the (12) strip and then circumcise to get:

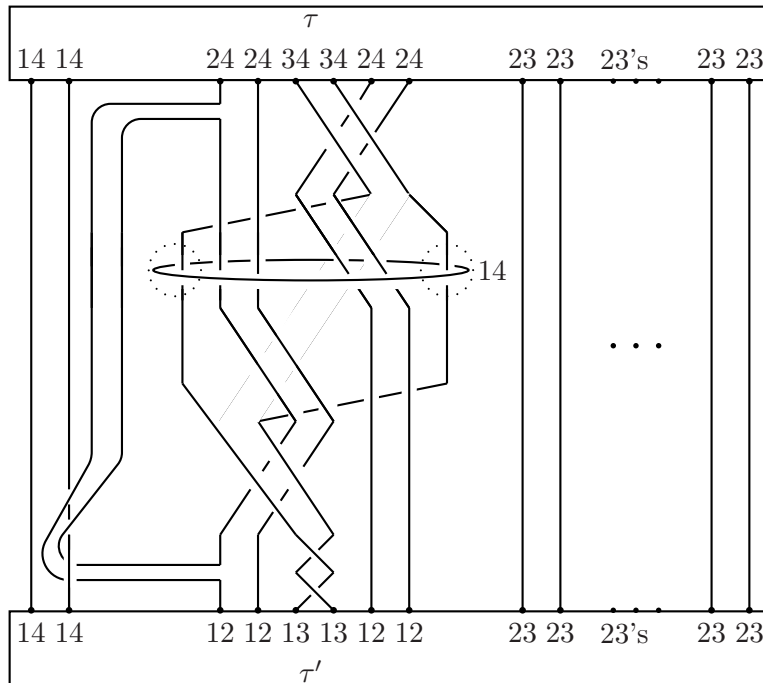


by isotopy and reverse circumcision. Now after moving the (14) circle beyond the (23) strands using move \mathcal{P} , flip it over the whole diagram, apply move \mathcal{X} , circumcise and isotope to complete move III.

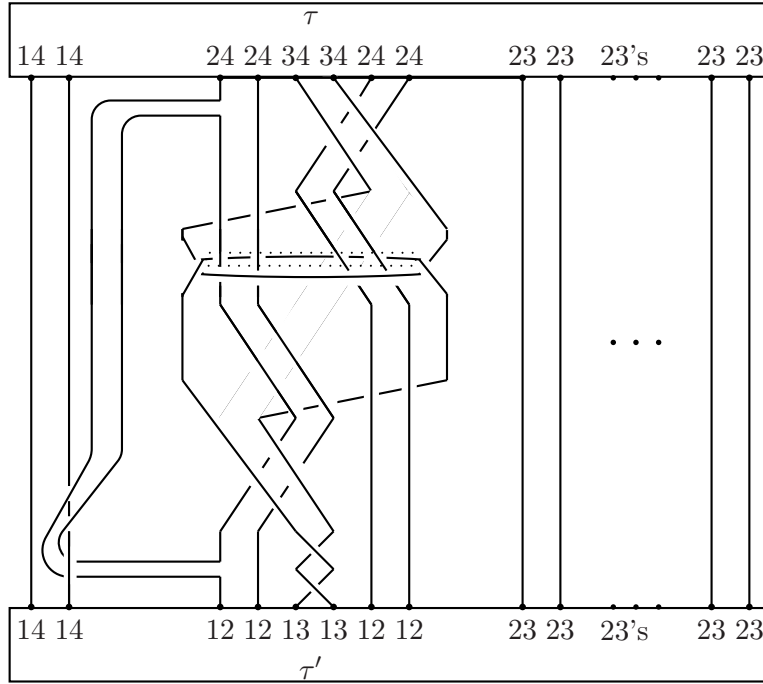
For move IV: Start again with isotopy and reverse circumcision to get:



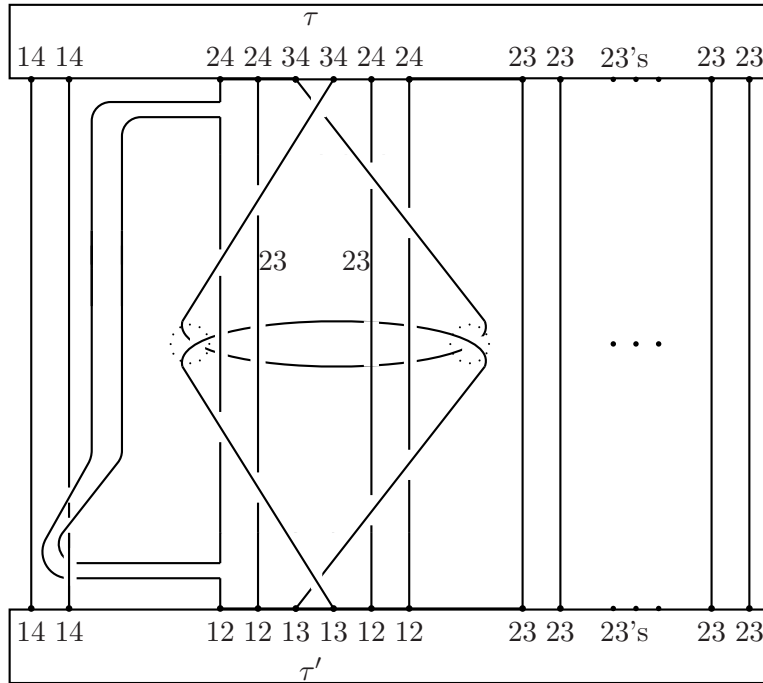
Then use move \mathcal{X} , isotopy and \mathcal{P} moves to get:



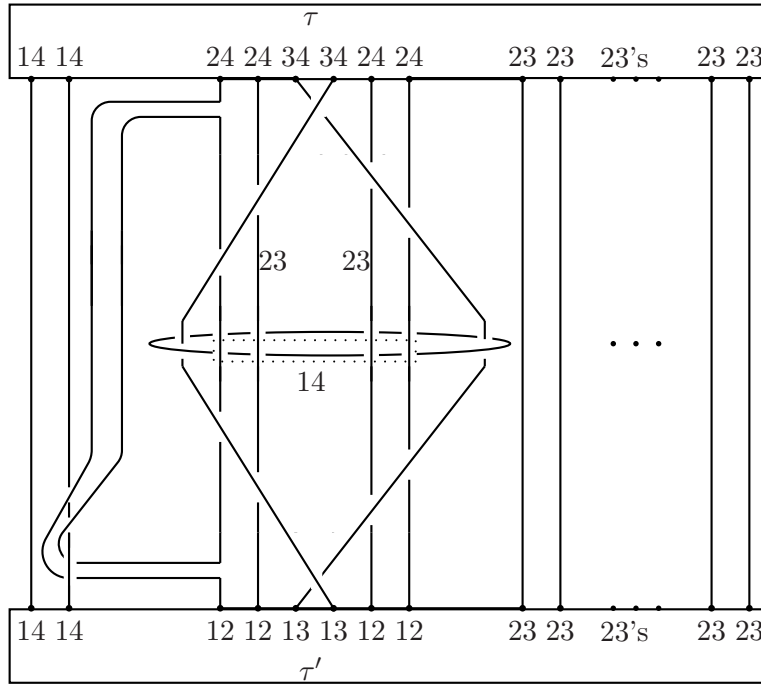
Then perform \mathcal{P} moves inside the dotted circles to get:



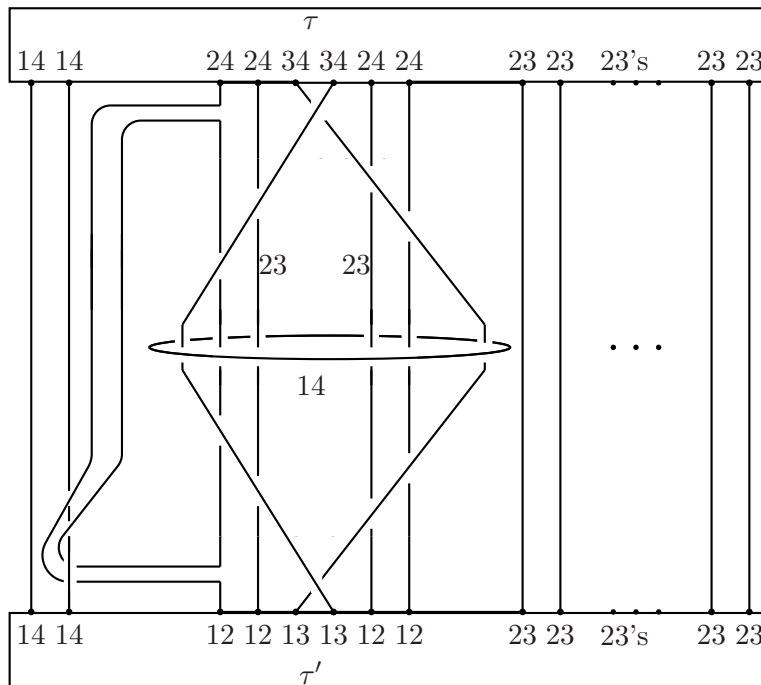
Then after changing all crossings inside the dotted rectangle using move \mathcal{P} isotopy:



Perform \mathcal{P} moves inside the dotted circles:



Perform \mathcal{P} moves inside the dotted rectangle:

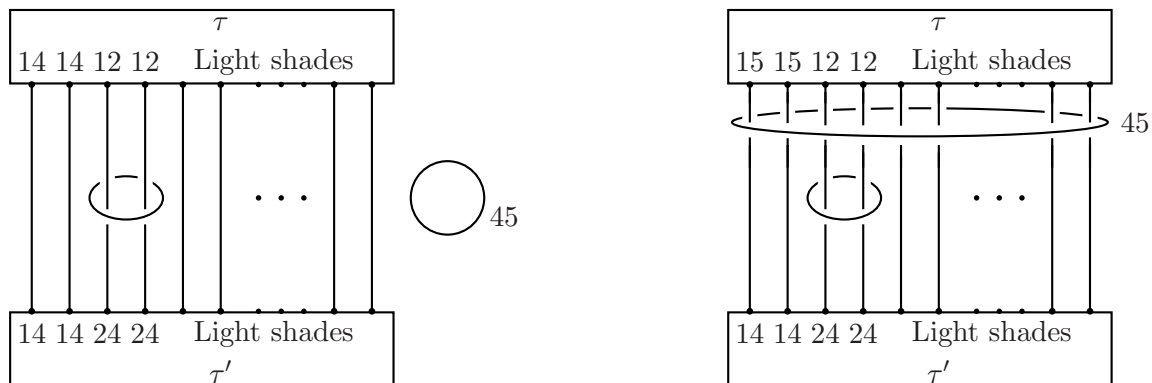


Now reverse the process starting from the second picture to complete move V.

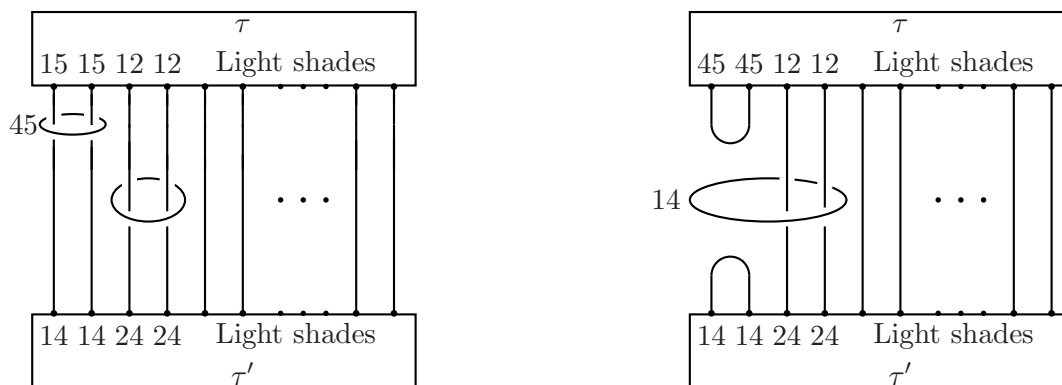
□

Proof of 4.2.2. It suffices to show that moves \mathcal{X} , II and IV can be realized:

For move \mathcal{X} , first add a trivial fifth sheet with monodromy (45) to get:

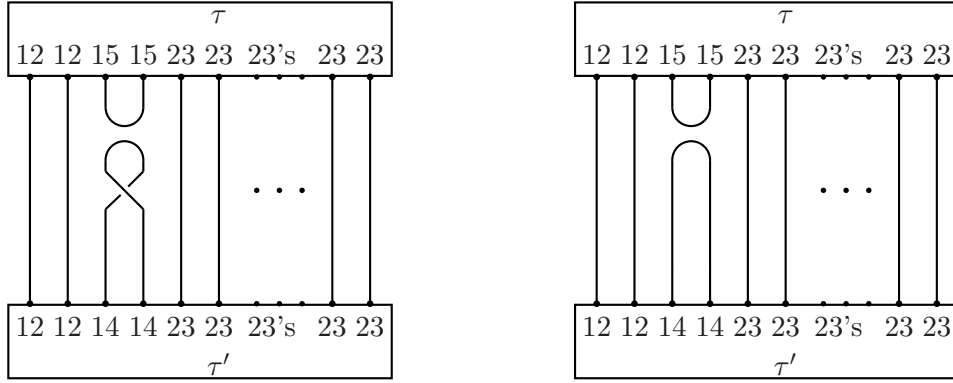


by isotopically flipping the trivial sheet over the whole diagram. Then apply a sequence of \mathcal{P} moves to get:



by circumcision and isotopy. Now isotopically push the (14) cup through the (14) circle and reverse the process to complete move \mathcal{X} .

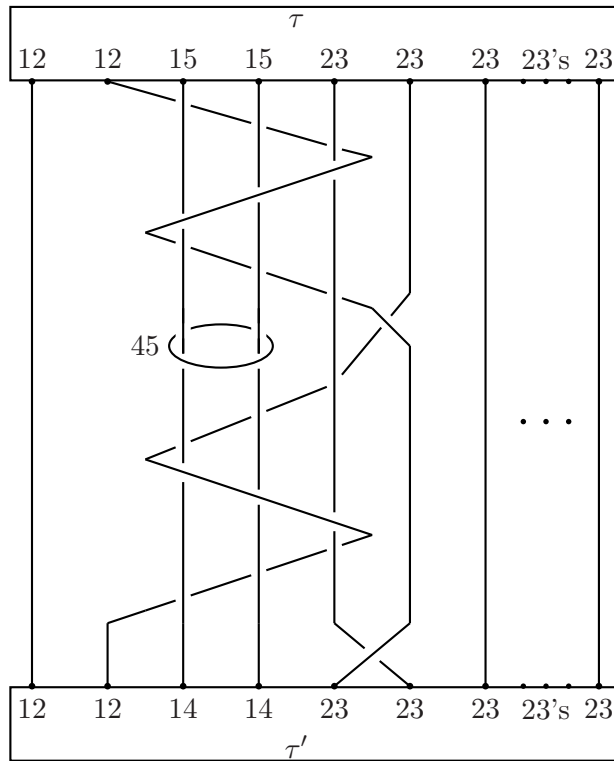
For move II: Add a trivial fifth sheet with monodromy (45) and after flipping it over the whole diagram, use \mathcal{P} moves and circumcision to get:



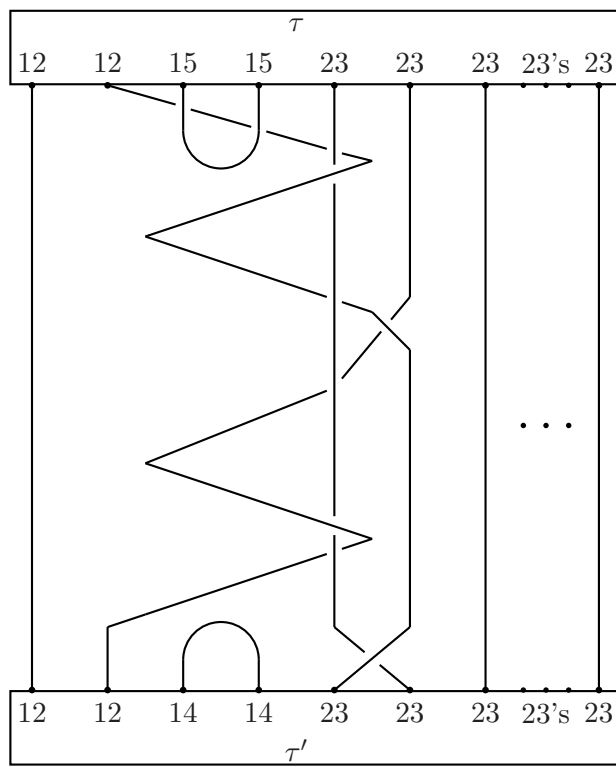
by isotopy. Now reverse the process to complete move II.

For move V:

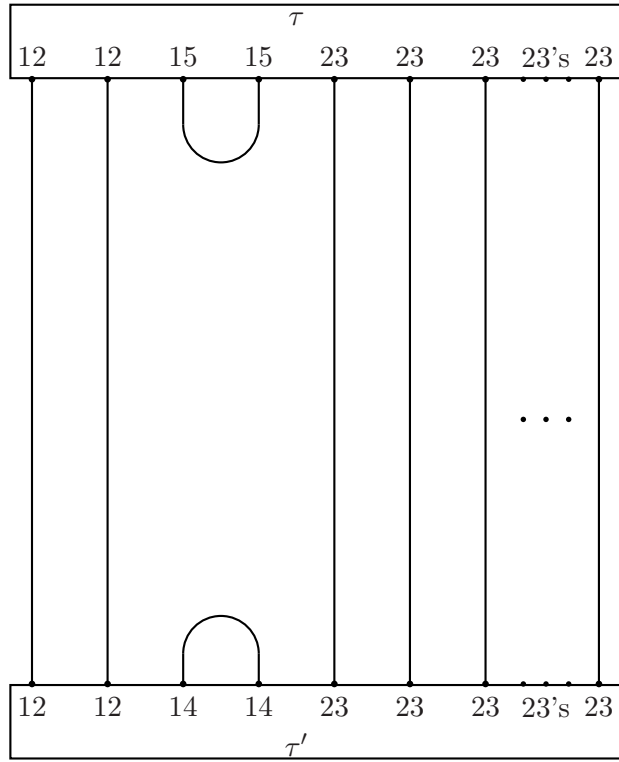
First add a trivial fifth sheet with monodromy (45), and then use isotopy and several \mathcal{P} moves to get:



Then circumcise and isotope to get:



Then apply two \mathcal{M} moves and isotopy to get:



From the last diagram apply reverse circumcision, \mathcal{P} moves, isotopy and erase the trivial sheet to complete move V.

This completes the proof of the theorem. □

5. SOME OPEN QUESTIONS

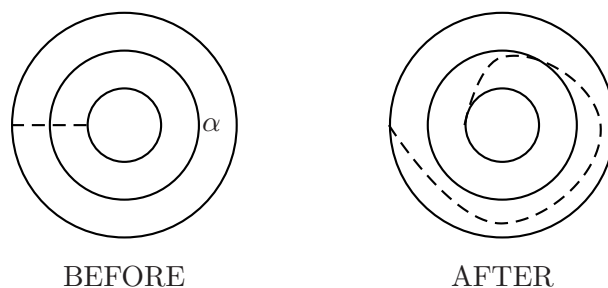
This work naturally suggests the following questions:

1. Is the fifth trivial sheet really necessary or are moves \mathcal{M} and \mathcal{P} enough by themselves? Equivalently can any bi-tricolored link be related to a tricolored link plus a trivial sheet, via moves \mathcal{M} and \mathcal{P} ?
2. More generally is there a degree m such that moves \mathcal{M} and \mathcal{P} are enough to related any two manifestations of the same 3-manifold as a simple m -sheeted branched covering of the three sphere?
3. [13] Are moves \mathcal{M} and \mathcal{P} plus addition/deletion of trivial sheets enough to relate any two manifestations of the same 3-manifold as a simple branched covering of the three sphere? Or, referring to the move of adding/deleting a trivial sheet as stabilization, are any two colored link presentations of the same 3-manifold stably equivalent?

APPENDIX A. WAJNRYB'S PRESENTATION OF \mathfrak{M}_g

Let Σ be an orientable surface. By the *mapping class group* $\mathfrak{M}(\Sigma)$ of Σ we mean the group of isotopy classes of orientation preserving homeomorphisms of Σ . $\mathfrak{M}(\Sigma)$ is indeed a group since it is the quotient of the group of orientation preserving homeomorphisms of Σ by the normal subgroup of homeomorphisms isotopic to identity.

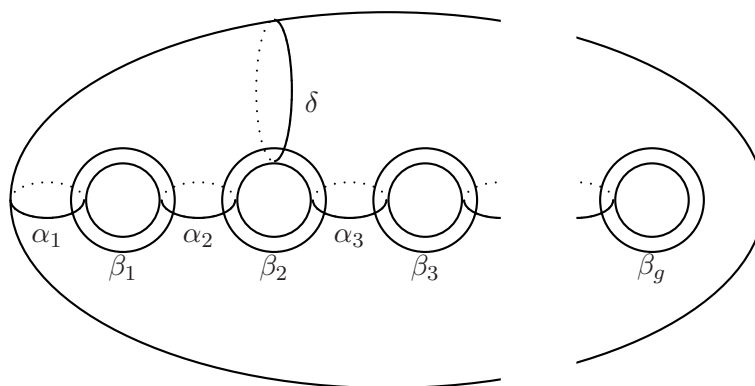
Definition A.0.5. Let α be a simple closed curve in Σ . A Dehn twist around α is a homeomorphism of Σ that is identity outside a tubular neighborhood of α and it is a full twist inside that neighborhood. More precisely if the tubular neighborhood of α is parameterized as $\{(r, \theta) | 1 \leq r \leq 2, \theta \in [0, 2\pi]\}$ with α being $\{r = 1\}$ then the map inside the tubular neighborhood is given by $(r, \theta) \mapsto (r, \theta + 2\pi r)$ (see Figure 32). The

FIGURE 32. A Dehn twist around α

isotopy class of a Dehn twist around α depends only on the isotopy class of α and is called *the* Dehn twist around α .

Curves in a surface are denoted by Greek letters and Dehn twists around them by the corresponding Latin letters.

The mapping class group of the standard genus g surface is denoted by \mathfrak{M}_g . Wajnryb gave the following presentation of \mathfrak{M}_g in [16].

FIGURE 33. The generators of \mathfrak{M}_g

Theorem A.0.6 (Wajnryb). *The mapping class group of \mathfrak{M}_g admits a presentation with generators $a_1, b_1, \dots, a_n, b_n, d$ (see Figure 33) and relations*

- (A) $a_i b_i a_i = b_i a_i b_i$, $a_{i+1} b_i a_{i+1} = b_i a_{i+1} b_i$, $b_2 d b_2 = d b_2 d$, and every other pair of generators commute.
- (B) $(a_1 b_1 a_2)^4 = d(b_2 a_2 b_1 a_1 a_1 b_1 a_2 b_2)^{-1} d b_2 a_2 b_1 a_1 a_1 b_1 a_2 b_2$.
- (C) $d t_2 d t_2^{-1} t_1 t_2 d (a_1 a_2 a_3 t_1 t_2)^{-1} = (u b_1 a_2 b_2 a_3 b_3)^{-1} v u b_1 a_2 b_2 a_3 b_3$ where $t_1 = b_1 a_1 a_2 b_1$, $t_2 = b_2 a_2 a_3 b_2$, $u = a_3 b_3 t_2 d (a_3 b_3 t_2)^{-1}$,
 $v = a_1 b_1 a_2 b_2 d (a_1 b_1 a_2 b_2)^{-1}$.
- (D) d_n commutes with $b_n a_n \cdots b_1 \cdots a_n b_n$ where

$$\begin{aligned} d_n &= (u_1 u_2 \cdots u_{n-1})^{-1} a_1 u_1 u_2 \cdots u_{n-1}, \\ u_i &= b_i a_{i+1} b_{i+1} v_i (b_{i+1} a_{i+1} b_i a_i)^{-1} \quad \text{for } i = 1, \dots, n-1, \\ v_1 &= (b_2 a_2 b_1 a_1 a_1 b_1 a_2 b_2)^{-1} d (b_2 a_2 b_1 a_1 a_1 b_1 a_2 b_2), \\ v_i &= t_{i-1} t_i v_{i-1} (t_{i-1} t_i)^{-1} \quad \text{for } i = 2, \dots, n-1, \\ t_i &= b_i a_i a_{i+1} b_i \quad \text{for } i = 1, \dots, n-1. \end{aligned}$$

APPENDIX B. BRAIDS

References for the material in this section are [3] and [6].

Definition B.0.7. Let $\text{Conf}_n(D^2)$ denote the configuration space of unordered n -tuples of distinct points of the 2-dimensional disc and chose a basepoint $L = \{A_0, \dots, A_{n-1}\}$. The fundamental group of $\text{Conf}_n(D^2)$ is called the braid group on n strands and is denoted by B_n , that is

$$B_n := \pi_1(\text{Conf}_n(D^2), L).$$

So a braid is (the homotopy class of) a closed path in $\text{Conf}_n(D^2)$. Such a path is equivalent to n nonintersecting paths in the disc with the property that the set of initial points and the set of endpoints are equal to L . We represent such an n -tuple of paths by n arcs in the solid cylinder $I \times D^2$, which are the graphs of the paths thought of as functions $I \rightarrow D^2$. We draw generic planar projections of braids with conventions analogous to the conventions for drawing links (see Appendix C).

Theorem B.0.8 (Artin). *For each $n \geq 1$ the braid group on n strands has the following presentation :*

$B_n = \langle \beta_0, \beta_1, \dots, \beta_{n-2} \mid \beta_i \beta_{i+1} \beta_i = \beta_{i+1} \beta_i \beta_{i+1} \text{ and } \beta_i \beta_j = \beta_j \beta_i \text{ if } |i - j| \geq 2 \rangle$,
 where β_i interchanges the i^{th} and $(i+1)^{\text{th}}$ strands as shown in Figure 34.

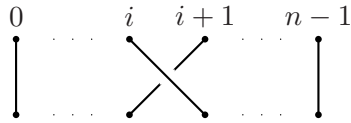


FIGURE 34. The generator β_i of B_n

APPENDIX C. LINK DIAGRAMS

Definition C.0.9. A *link* L is a 1-dimensional submanifold of the three sphere S^3 . A *knot* is a connected link.

Two links L, L' are called isotopic if there is an ambient isotopy carrying one to the other, that is there is a homotopy $h_t : S^3 \longrightarrow S^3, 0 \leq t \leq 1$ with the properties:

- $h_0 = \text{id}$
- $\forall t, h_t$ is a homeomorphism.
- $L' = h_1(L)$

The fundamental group of the complement of L is called the group of the link L .

Isotopic links have isomorphic groups, and furthermore an isotopy between links induces an isomorphism between link groups.

A link is usually represented by drawing its image under a generic (i.e. with only double points) projection onto a plane. Furthermore at each double point of such a diagram the relative distance of the two points from the plane of projection is recorded by drawing the nearest piece broken as in Figure 35. (See any book in knot theory, for example [14].) The double points of such a diagram (called *link diagram*) are called *crossings*. A link diagram is thus broken into connected pieces called the *arcs* of the diagram.



FIGURE 35. A crossing

Theorem C.0.10. *Two diagrams represent isotopic links iff they can be related via planar isotopy and a finite number of Reidemeister moves $R1, R2$ and $R3$ shown in Figure 36.*

Given a diagram of a link there is an associated presentation (called the Wirtinger presentation) of the link group obtained as follows:

Generators There is one generator for each arc of the diagram representing a lasso that goes around that arc.

Relations There is one relation at each crossing asserting that the (generator corresponding to) the over arc conjugates one of the under arcs to the other.

Remark C.0.11. See [14] for a precise statement of the conjugation relations. For the purposes of this work the above vague description is enough.

Remark C.0.12. Notice that one can get a precise description of the isomorphism between link groups induced by an isotopy by tracing how the Wirtinger presentation changes under Reidemeister moves.

APPENDIX D. HEEGAARD SPLITTINGS

Definition D.0.13. Let M be a 3-manifold with boundary ∂M . We say that a manifold M' is obtained by M by attaching a 1-handle iff M' is homeomorphic to the space obtained

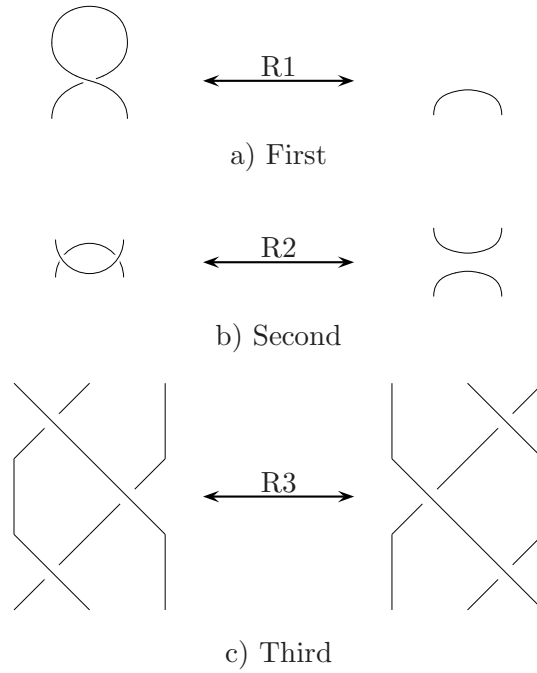


FIGURE 36. The Reidemeister moves

by attaching a “solid cylinder”, $I \times D^2$ to M via a map

$$\{0, 1\} \times D^2 \longrightarrow \partial M$$

where $\{0, 1\} = \partial I$.

Definition D.0.14. A (3-dimensional) handlebody H is a 3-manifold obtained by attaching some 1-handles to the 3-ball D^3 . The genus of H is the genus of the surface ∂H .

Definition D.0.15. A genus g Heegaard splitting of a closed orientable 3-manifold M is a decomposition

$$M = H_1 \bigcup_{\phi} H_2$$

where H_1 and H_2 are genus g handlebodies and ϕ , called the splitting homeomorphism, is a homeomorphism $\phi : \partial H_1 \longrightarrow \partial H_2$.

Two Heegaard splittings $H_1 \bigcup_{\phi} H_2$ and $H'_1 \bigcup_{\phi'} H'_2$ are called equivalent if there exist homeomorphisms f_1, \bar{f}_1 and f_2, \bar{f}_2 so that the following diagram commutes:

$$\begin{array}{ccccc} H_1 & \supset & \partial H_1 & \xrightarrow{\phi} & \partial H_2 & \subset & H_2 \\ \bar{f}_1 \downarrow & & f_1 \downarrow & & \downarrow f_2 & & \downarrow \bar{f}_2 \\ H'_1 & \supset & \partial H'_1 & \xrightarrow{\phi'} & \partial H'_2 & \subset & H'_2 \end{array}$$

Theorem D.0.16. *Every closed orientable 3-manifold M admits a Heegaard splitting.*

Sketch of proof. M admits a triangulation. Take a triangulation of M and observe that M is the union of thickenings of the 1-skeleton of this triangulation and the 1-skeleton of the dual cellular decomposition. Both thickenings are handlebodies. See [14] for details. \square

Of course the same manifold admits many Heegaard splittings. For example given Heegaard splittings of two manifolds M_1 and M_2 there is a connected sum Heegaard splitting of the connected sum $M_1 \# M_2$. Therefore taking connected sums with splittings of the 3-sphere produces new splittings of the same manifold. Theorem D.0.18 below asserts that essentially this is all that can happen.

Definition D.0.17. The *standard* genus 1 splitting of the 3-sphere is the following:

$$S^3 = S^1 \times D^2 \bigcup_{S^1 \times S^1} D^2 \times S^1.$$

That is the splitting of S^3 as two solid tori (genus 1 handlebodies) glued via the map of the torus $S^1 \times S^1$ to itself that interchanges the coordinates.

Taking connected sum with the standard genus 1 splitting of S^3 is referred to as *stabilization*.

Theorem D.0.18. *Any two Heegaard splittings of the same 3-manifold are stably equivalent, that is they become equivalent after enough stabilizations. We emphasize that usually both splittings need to be stabilized before they become equivalent.*

Proof. See [17]. \square

REFERENCES

- [1] J. W. Alexander, *Note on Riemann spaces*, Bull. Amer. Math. Soc. **26** (1920), pp. 370-372.
- [2] I. Bernstein and A. Edmonds, *On the construction of branched coverings of low-dimensional manifolds*, Trans. of Amer. Math. Soc., **247** (1979), 87-124.
- [3] J. S. Birman, *Braids, links, and mapping class groups*, Annals of Math. Studies, No. 82, Princeton University Press, Princeton New Jersey, 1974.
- [4] J. S. Birman and B. Wajnryb, *3-Fold branched coverings and the mapping class group of a surface*, Geometry and Topology, Lecture Notes in Math., vol 1167, Springer-Verlag, Berlin and New York, 1985, pp.24-46.
- [5] J. S. Birman and B. Wajnryb, *Errata: Presentations of the mapping class groups*, Israel J. of Math. **88** (1994), 425-427.
- [6] G. Brude and H. Zieschang, *Knots*, De Gruyter studies in Math. 5, De Gruyter, 1985.
- [7] R. Fox, *Covering spaces with singularities in Algebraic geometry and topology, a symposium in honor of S. Lefschetz* (Ed. by Fox, Spencer, and Tucker), Princeton 1957, 243-257.
- [8] H. M. Hilden, *Every closed orientable 3-manifold is a 3-fold branched covering space of S^3* , Bull. Amer. Math. Soc. **80** (1974), 1243-1244.
- [9] J. M. Montesinos, *A representation of closed orientable 3-manifolds as 3-fold branched coverings of S^3* , Bull. Amer. Math. Soc. **80** (1974), 845-846.
- [10] J. M. Montesinos, *A note on moves and irregular coverings of S^4* , Contemp. Math. **44** (1985) 345-349.
- [11] R. Piergallini, *Covering moves*, Trans. Amer. Math. Soc. **325** (1991), 903-920.
- [12] R. Piergallini, *Four-manifolds as 4-fold branched coverings of S^4* , Topology **34** No 3 (1995), 497-508.
- [13] R. Piergallini, Private Communication.
- [14] D. Rolfsen, *Knots and Links*, Publish or Perish, 1976.
- [15] S. Suzuki, *On homeomorphisms of a 3-dimensional handlebody*, Canad. J. Math. **29** (1977), 111-124.
- [16] B. Wajnryb, *A simple presentation of the mapping class group of an orientable surface*, Israel J. of Math **45** (1983), 157-174.
- [17] F. Waldhausen, *Heegaard-Zerlegungen der 3-Sphäre*, Topology **7** (1968), 195-203.
- [18] H. Zieschang and E. Vogt and H. Coldway, *Surfaces and Planar Discontinuous Groups*, Lecture Notes in Math., vol 835 ,Springer-Verlag, Berlin Heidelberg New York, 1980.

DEPARTMENT OF MATHEMATICS, UNIVERSITY OF CALIFORNIA, RIVERSIDE CA 92521
E-mail address: `nea@math.ucr.edu`